*Semiconductor Physics, Quantum Electronics & Optoelectronics, 2012. V. 15, N 2. P. 91-116.*

PACS 72.20.Jv, 73.40.Cg, 84.60.Jt, 85.30.De

# Efficiency a-Si:H solar cell. Detailed theory

**Yu.V. Kryuchenko, A.V. Sachenko, A.V. Bobyl, V.P. Kostylyov, P.N. Romanets, I.O. Sokolovskyi, A.I. Shkrebtii, E.I. Terukov**
*V. Lashkaryov Institute of Semiconductor Physics, NAS of Ukraine*
*41, prospect Nauky, 03028 Kyiv, Ukraine*

**Abstract.** We develop a detailed formalism to photoconversion efficiency $\eta$ of hydrogenated amorphous silicon (a-Si:H) based solar cells with a contact grid. This efficient three-dimensional model allows firstly optimization of the $p^{+}-i-n$ sandwich in terms of carrier mobilities, thickness of the layers, doping levels and others. Secondly, geometry of the grid fingers that conduct the photocurrent to the bus bars and ITO/$SiO_2$ layers has been optimized, and the effect of non-zero sun beam incidence angles has been included as well. The model allows optimization of the amorphous Si based solar cells in a wide range of key parameters.

**Keywords:** photoconversion efficiency, hydrogenated amorphous silicon, a-Si:H solar cells.

Manuscript received 05.03.12; revised version received 20.03.12; accepted for publication 27.03.12; published online 15.05.12.

## 1. Introduction

Thin film hydrogenated amorphous silicon (a-Si:H) is widely used for photovoltaic applications. Amorphous silicon-based solar cells (SC) are very promising because of low production cost, possibility of covering large uneven areas, and sufficiently high efficiency. In order to get the best possible performance of the a-Si:H solar cells, it is important to (i) produce a high quality amorphous films with $p-i-n$ junction, and (ii) optimize the films and solar cells in terms of their parameters such as, for instance, *p*-, *i*- and *n*-layer thicknesses, their doping levels, electron and hole mobilities $\mu_n$ and $\mu_p$ and their lifetime, resistance of *p*-, *i*- and *n*-layers, contact grid geometry and parameters of the transparent conducting and antireflecting layers. In this paper, we propose a detailed theory of photoconversion in the structures of a-Si:H, taking into account the dependence of the efficiency of a sufficiently large number of physical parameters.

## 2. Model of an active region in the a-Si:H solar cell

In the case when no external (irradiation) excitation of electrons and holes in a system occurs and electron-hole recombination channels are totally absent, the following standard continuity equation for carriers in the system is valid:

$$\frac{dp}{dt} + \nabla \cdot \boldsymbol{I}_p = 0, \qquad (1)$$

where $p$ is the particle concentration and $\boldsymbol{I}_p$ – particle flux.

If processes of generation and recombination of particles are taken into account, then Eq. (1) takes a more complicated form of generation-recombination balance equation, namely:

$$\frac{dp}{dt} = g_p - \frac{p - p_0}{\tau_p} - \frac{1}{e}\nabla \cdot \boldsymbol{j}_p \qquad (2)$$

for holes and

$$\frac{dn}{dt} = g_n - \frac{n - n_0}{\tau_n} + \frac{1}{e}\nabla \cdot \boldsymbol{j}_n \qquad (3)$$

© 2012, V. Lashkaryov Institute of Semiconductor Physics, National Academy of Sciences of Ukraine

for electrons, where $g_p$ and $g_n$ are the generation rates ($g_p = g_n = g$ for generation by external irradiation, when each absorbed photon with an energy higher than band gap energy creates simultaneously an electron in the conduction band and a hole in the valence band), $p_0$ and $n_0$ are the equilibrium hole and electron concentrations in a system without external excitation, $\tau_p$ and $\tau_n$ are the hole and electron lifetimes, $\boldsymbol{j}_p$ and $\boldsymbol{j}_n$ are the densities of hole and electron currents, which in turn can be written as

$$\boldsymbol{j}_p = e(\boldsymbol{E}\mu_p p - D_p \nabla p) \quad (4)$$

and

$$\boldsymbol{j}_n = e(\boldsymbol{E}\mu_n n + D_n \nabla n), \quad (5)$$

where $\boldsymbol{E}$ is the electric field, $\mu_{p(n)}$ are the hole (electron) mobilities, $D_{p(n)}$ are the corresponding diffusion coefficients. Accounting for Einstein relation $D_{p(n)} = \frac{kT}{e}\mu_{p(n)}$ and expressing electric field $\boldsymbol{E}$ in the system via potential $\varphi$, $E = -\nabla\varphi$, Eqs. (4) and (5) take up the following form:

$$\frac{\boldsymbol{i}_h}{D_p} = -p\nabla y - \nabla p \quad (6)$$

and

$$\frac{\boldsymbol{i}_e}{D_n} = -n\nabla y + \nabla n, \quad (7)$$

where $y = e\varphi / kT$ is the dimensionless potential energy of positive charge, $\boldsymbol{i}_h = \boldsymbol{j}_p / e$ and $\boldsymbol{i}_e = \boldsymbol{j}_n / e$ are the fluxes of positive charges, corresponding to movement of holes and electrons in the system. Substituting (6) and (7) into (2) and (3), we obtain at steady-state conditions ($dp/dt = dn/dt = 0$) in the case of one-dimensional system (which is the subject of our subsequent consideration) the following equations:

$$\frac{d^2 p}{dz^2} - \frac{p - p_0}{L_p} + \frac{dy}{dz}\frac{dp}{dz} + p\frac{d^2 y}{dz^2} = -\frac{g(z)}{D_p}, \quad (8)$$

$$\frac{d^2 n}{dz^2} - \frac{n - n_0}{L_n} - \frac{dy}{dz}\frac{dn}{dz} - n\frac{d^2 y}{dz^2} = -\frac{g(z)}{D_n}, \quad (9)$$

where $L_p = \sqrt{D_p \tau_p}$ is the hole diffusion length, $L_n = \sqrt{D_n \tau_n}$ is the electron diffusion length, $z$ is the coordinate in the direction normal to structure surface.

Further, by calculating short-circuit current in the system, we consider the active region of a-Si:H solar cell as being formed during its growth by two main layers (see Fig. 1), namely: i) doped $p^+$-layer (with the layer thickness $d_p$) adjacent to the front surface and ii) more deep undoped (or slightly doped with donors) $i(n)$-layer with the layer thickness $d$. Besides, technological $n^+$ layer also is formed in practice at rear surface to have good rear contact properties, but its thickness $d_n$ is usually too small to influence the charge generation and collection, so in the first approximation it can be excluded from the consideration that concerns short-circuit current formation. Considering physical properties of the active a-Si:H region, it is convenient to divide this region into three physically different parts: I) $p^+$-layer with the thickness $d_p - z_p$. It is simply a part of technologically formed $p^+$-layer that lies outside the SCR arising at $p^+ - i(n)$ junction. In this region, excess electrons contribute to short-circuit current. II) $i(n)$-layer with the thickness $d - z_n$. It is $i(n)$-part of a-Si:H that lies outside SCR region. In this region, excess holes form corresponding contribution into short-circuit current. III) Third layer is the SCR itself in the vicinity of $z = d_p$. The thickness of SCR equals to $z_p + z_n$. At short-circuit current conditions, the band bending in SCR becomes practically the same as in dark conditions (i.e. when generation of mobile electrons and holes by external irradiation is turned off). For this reason, in the SCR rather high electric field exists, so the electrons and holes generated in this region are quickly separated from each other by the field, and in the first approximation their movement can be considered neglecting their recombination. Contrary, in layers I and II outside SCR region, the electric field is enough low in these conditions, so we can neglect it in the first approximation.

It follows from the written above that a problem of short-circuit current collection in a-Si:H can be solved by separately considering the regions $0 < z < d_p - z_p$ and $d_p + z_n < z < d_p + d$ with appropriate boundary conditions.

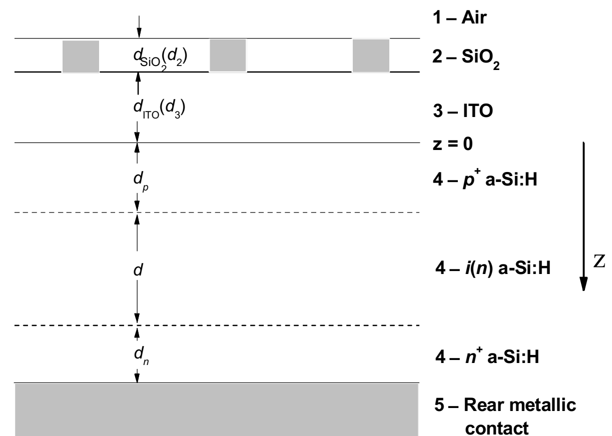


**Fig. 1.** Schematic view of a-Si:H solar cell structure.

© 2012, V. Lashkaryov Institute of Semiconductor Physics, National Academy of Sciences of Ukraine

### 3. Short-circuit current collection from $p^+$-region in a-Si:H layer

In the region I, where excess minor carriers (electrons) contribute to the short-circuit current, the equation (9) in diffusion approximation (drift terms are small enough as compared to the diffusion ones) takes up the following form:

$$\frac{d^2\Delta n^{p(s)}}{dz^2} - \frac{\Delta n^{p(s)}}{L_n^2} = -\frac{g^{p(s)}(z)}{D_n} , \qquad (10)$$

where $\Delta n^{p(s)}(z) = n^{p(s)}(z) - n_0$. Superscripts $p(s)$ in the generation term $g(z)$ and excess electron concentration $\Delta n(z)$ are introduced to account for two possible independent polarizations of the incident light because in the case of its oblique incidence, when the angle of light incidence differs from zero, reflection and transmission coefficients for the light polarized in the plane of incidence ($p$-polarized portion of incident light) differ from those for light polarized in parallel to SC surface ($s$-polarized portion of incident light). In the generation term $g^{p(s)}(z)$, all the contributions from the total spectrum of the incident light are present, so generally it is not monochromatic. However, in linear approximation, the problem can be considered separately for each constituting (monochromatic) part of the total spectrum inherent to incident irradiation, and total concentrations as well as short-circuit currents can be found by summing the contributions from the constituting parts of the spectrum. For this reason, we consider further a particular case of monochromatic irradiation with the wavelength λ.

Uniform solution of Eq. (10), to which zero right-hand part of the equation corresponds, can be expressed as $C_{1,n}^{p(s)} \exp(-z/L_n) + C_{2,n}^{p(s)} \exp(z/L_n)$. General solution of Eq. (10) is a sum of the uniform solution and the partial one, defined by the generation term in the right-hand side of the equation. If possible multiple internal reflections of the light transmitted into a-Si:H layer from a-Si:H layer boundaries are taken into account, then the generation term $g^{p(s)}(z,\lambda)$ is expressed as

$$g^{p(s)}(z,\lambda) = \frac{(1-m)\,\alpha_\lambda\, I_0^{p(s)}(\lambda)\, T_{1\to 4}^{p(s)}(\lambda)}{1 - R_{4\to 1}^{p(s)}(\lambda)\, R_{4\to 5}^{p(s)}(\lambda) \exp\left[-2\alpha_\lambda (d_p + d + d_n)\right]} \times$$
$$\times \left\{\exp(-\alpha_\lambda z) + R_{4\to 5}^{p(s)}(\lambda) \exp[-2\alpha_\lambda (d_p + d + d_n)] \exp(\alpha_\lambda z)\right\}, \qquad (11)$$

where $\alpha_\lambda$ is the absorption coefficient of a-Si:H material at the wavelength λ, $m$ – relative metallization of the front surface by finger electrodes (the part of the front SC surface, which is covered by the electrodes, produces corresponding shade in active region), $I_0^{p(s)}(\lambda)$ – irradiating light intensity at the wavelength λ. For simplicity, we denote by indices *1* to *5* all optically different media, which determine the incident irradiation transmission and reflection (see Fig. 1) in the SC, so that $T_{1\to 4}^{p(s)}(\lambda)$ is the transmission coefficient for $p(s)$-polarized light incident from air (medium *1*) onto SC front surface, which determines corresponding irradiation transmission into active a-Si:H region (medium *4*) of SC with account of multiple intermediate light reflections and transmissions at the interfaces 1/2, 2/3 and 3/4, $R_{4\to 1}^{p(s)}(\lambda)$ is the reflection coefficient for the light incident from a-Si:H region (medium *4*) onto 3/4 interface which accounts for the analogous multiple light reflections and transmissions at the interfaces 1/2, 2/3 and 3/4, $R_{4\to 5}^{p(s)}(\lambda)$ is the reflection coefficient for the light incident from a-Si:H region (medium *4*) onto rear metallic contact (medium *5*).

In accordance with the explicit form of generation term (11), general solution of Eq. (10) takes up the following form:

$$\begin{pmatrix} \Delta n_\lambda(z) \\ d\Delta n_\lambda / dz \end{pmatrix}^{p(s)} =$$
$$= C_{1,n}^{\lambda,p(s)} \exp(-z/L_n) \begin{pmatrix} 1 \\ -1/L_n \end{pmatrix} + C_{2,n}^{\lambda,p(s)} \exp(z/L_n) \begin{pmatrix} 1 \\ 1/L_n \end{pmatrix} +$$
$$+ A_{1,n}^{\lambda,p(s)} \exp(-\alpha_\lambda z) \begin{pmatrix} 1 \\ -\alpha_\lambda \end{pmatrix} + A_{2,n}^{\lambda,p(s)} \exp(\alpha_\lambda z) \begin{pmatrix} 1 \\ \alpha_\lambda \end{pmatrix}, \qquad (12)$$

where $C_{1,n}^{\lambda,p(s)}$ and $C_{2,n}^{\lambda,p(s)}$ are the coefficients, which has to be determined from boundary conditions,

$$A_{1,n}^{\lambda,p(s)} = \frac{(1-m)\,\alpha_\lambda\, I_0^{p(s)}(\lambda)\, T_{1\to 4}^{p(s)}(\lambda)}{1 - R_{4\to 1}^{p(s)}(\lambda)\, R_{4\to 5}^{p(s)}(\lambda) \exp\left[-2\alpha_\lambda (d_p + d + d_n)\right]} \times$$
$$\times \frac{L_n^2 / D_n}{1 - (\alpha_\lambda L_n)^2} ,$$
$$A_{2,n}^{\lambda,p(s)} = A_{1,n}^{\lambda,p(s)}\, R_{4\to 5}^{p(s)}(\lambda) \exp\left[-2\alpha_\lambda (d_p + d + d_n)\right] . \qquad (13)$$

First boundary condition can be written in the form of standard balance equation for excess electron fluxes through front a-Si:H surface (interface) at $z = 0$ (see Fig. 1):

$$D_n \left.\frac{d\Delta n_\lambda^{p(s)}}{dz}\right|_{z=0} = S_0\, \Delta n_\lambda^{p(s)}(0) , \qquad (14)$$

where $S_0$ is the surface recombination rate for electrons. To obtain the second boundary condition at $z = d_p - z_p$, we consider SCR region neglecting electron-hole recombination. In this approximation, Eq. (3) takes up the following form:

$$\frac{di_e^{\lambda,p(s)}}{dz} = -g^{p(s)}(z,\lambda) , \qquad (15)$$

© 2012, V. Lashkaryov Institute of Semiconductor Physics, National Academy of Sciences of Ukraine

where flux $i_e^{\lambda,p(s)}$ is expressed by formula (7), which in 1D case can be rewritten as:

$$\frac{dn_\lambda^{p(s)}}{dz} - n_\lambda^{p(s)}\frac{dy}{dz} = \frac{i_e^{\lambda,p(s)}}{D_n}. \quad (16)$$

In equilibrium conditions, when $i_e^{\lambda,p(s)} = 0$, solution of the latter equation is the well-known equilibrium one:

$$n_\lambda^{p(s)}(z) \equiv n_0(z) = n_n \exp[y(z)], \quad (17)$$

where $n_n$ is the electron concentration in $i(n)$-region beyond SCR layer, where electrons are the majority carriers. At irradiation, when $i_e^{\lambda,p(s)} \neq 0$, solution of Eq. (16) can be found in the form of

$$n_\lambda^{p(s)}(z) = B_n^{\lambda,p(s)}(z)\exp[y(z)]. \quad (18)$$

Substituting (18) into Eq. (16), we obtain the following equation for the coefficient $B_n^{\lambda,p(s)}$:

$$\frac{dB_n^{\lambda,p(s)}}{dz} = \exp[-y(z)]i_e^{\lambda,p(s)}(z)/D_n. \quad (19)$$

General solution of this equation can be written as

$$B_n^{\lambda,p(s)}(z) = B_{n0} + \frac{1}{D_n}\int_{z_0}^{z}\exp[-y(z')]i_e^{\lambda,p(s)}(z')\,dz', \quad (20)$$

where $B_{n0}$ and $z_0$ are two arbitrary constants. Substituting (20) into (18), we obtain following expression for $n_\lambda^{p(s)}(z)$ in the SCR region:

$$n_\lambda^{p(s)}(z) = \\ = \exp[y(z)]\left\{n_n + \frac{1}{D_n}\int_{d_p+z_n}^{z}\exp[-y(z')]\,i_e^{\lambda,p(s)}(z')\,dz'\right\}, \quad (21)$$

where explicit values of $B_{n0}$ and $z_0$ are chosen to provide the right value $n_\lambda^{p(s)}(z) = n_n$ at $z = d_p + z_n$ (no accumulation of excess electrons is supposed in a-Si:H $i(n)$-region beyond SCR layer at short-circuit current conditions, i.e. all electrons supplied by $p$-region in $i(n)$-region and generated in $i(n)$-region pass away to rear contact or recombine with holes, so that electron concentration in this region remains practically equilibrium one).

By substitution Eq. (11) into Eq. (15), the following explicit expressions for the flux $i_e^{\lambda,p(s)}$ in SCR can be written:

$$i_e^{\lambda,p(s)}(z) = i_e^{\lambda,p(s)}(d_p - z_p) - \\ -\tilde{A}_1^{\lambda,p(s)}\exp[-\alpha_\lambda(d_p - z_p)]\{1 - \exp[-\alpha_\lambda(z - d_p + z_p)]\} + \\ + \tilde{A}_2^{\lambda,p(s)}\exp[\alpha_\lambda(d_p - z_p)]\{1 - \exp[\alpha_\lambda(z - d_p + z_p)]\}, \quad (22)$$

where

$$\tilde{A}_1^{\lambda,p(s)} = \frac{(1-m)\;I_0^{p(s)}(\lambda)\,T_{1\to4}^{p(s)}(\lambda)}{1 - R_{4\to1}^{p(s)}(\lambda)\,R_{4\to5}^{p(s)}(\lambda)\exp\left[-2\alpha_\lambda(d_p + d + d_n)\right]} \quad (23)$$

and

$$\tilde{A}_2^{\lambda,p(s)} = \\ \frac{(1-m)\;I_0^{p(s)}(\lambda)\,T_{1\to4}^{p(s)}(\lambda)\,R_{4\to5}^{p(s)}(\lambda)\exp[-2\alpha_\lambda(d_p + d + d_n)]}{1 - R_{4\to1}^{p(s)}(\lambda)\,R_{4\to5}^{p(s)}(\lambda)\exp\left[-2\alpha_\lambda(d_p + d + d_n)\right]}. \quad (24)$$

As it follows from Eq. (21), at the SCR boundary $z = d_p - z_p$

$$n_\lambda^{p(s)}(d_p - z_p) - n_n\exp(-y_{pn}) \equiv \Delta n_\lambda^{p(s)}(d_p - z_p) = \\ = \frac{\exp(-y_{pn})}{D_n}\int_{d_p+z_n}^{d_p-z_p}\exp[-y(z)]\,i_e^{\lambda,p(s)}(z)\,dz, \quad (25)$$

where $y_{pn} = |\,y(d_p - z_p)\,|$ is the absolute value of total band bending in the SCR region in $kT$ units ($y = 0$ in $i(n)$-region of a-Si:H layer at $z \geq d_p + z_n$). Taking into account that according to (7) the flux $i_e^{\lambda,p(s)}$ at the SCR boundary $z = d_p - z_p$ in the formula (22) can be expressed as

$$i_e^{\lambda,p(s)}(d_p - z_p) = D_n\left.\frac{d\Delta n_\lambda^{p(s)}}{dz}\right|_{z=d_p-z_p}, \quad (26)$$

two boundary conditions (14) and (25) can be rewritten in the form of the following two explicit algebraic equations for the coefficients $C_{1,n}^{\lambda,p(s)}$ and $C_{2,n}^{\lambda,p(s)}$:

$$C_{1,n}^{\lambda,p(s)}(S_0 + V_n) + C_{2,n}^{\lambda,p(s)}(S_0 - V_n) = \\ = -A_{1,n}^{\lambda,p(s)}(\alpha_\lambda D_n + S_0) + A_{2,n}^{\lambda,p(s)}(\alpha_\lambda D_n - S_0), \quad (27)$$

$$C_{1,n}^{\lambda,p(s)}\exp[-(d_p - z_p)/L_n]\,(1 - I_{y-}) + \\ + C_{2,n}^{\lambda,p(s)}\exp[(d_p - z_p)/L_n]\,(1 + I_{y-}) = \\ = A_{1,n}^{\lambda,p(s)}\left\{\exp[-\alpha_\lambda(d_p - z_p)]\left[\frac{I_{y-}}{\alpha_\lambda L_n} - 1\right] - \frac{1-(\alpha_\lambda L_n)^2}{\alpha_\lambda L_n}I_{y-}^{\alpha_\lambda -}\right\} + \\ + A_{2,n}^{\lambda,p(s)}\left\{-\exp[\alpha_\lambda(d_p - z_p)]\left[\frac{I_{y-}}{\alpha_\lambda L_n} + 1\right] + \frac{1-(\alpha_\lambda L_n)^2}{\alpha_\lambda L_n}I_{y-}^{\alpha_\lambda +}\right\}, \quad (28)$$

where $V_n = D_n / L_n$, $I_{y-} = \int_{d_p-z_p}^{d_p+z_n}\exp[-y(z) - y_{pn}]\,dz / L_n$,

$$I_{y-}^{\alpha-} = \int_{d_p-z_p}^{d_p+z_n}\exp[-y(z) - y_{pn} - \alpha z]\,dz / L_n,$$

$$I_{y-}^{\alpha+} = \int_{d_p-z_p}^{d_p+z_n}\exp[-y(z) - y_{pn} + \alpha z]\,dz / L_n.$$

© 2012, V. Lashkaryov Institute of Semiconductor Physics, National Academy of Sciences of Ukraine

Thus, calculating the coefficients $C_{1,n}^{\lambda,p(s)}$ and $C_{2,n}^{\lambda,p(s)}$ from the system of algebraic equations (27) and (28), we completely determine the electron component of the density of short-circuit current $j_{e,SC}^{\lambda,p(s)}$:

$$j_{e,SC}^{\lambda,p(s)} \equiv e i_e^{\lambda,p(s)}(d_p - z_p) =$$
$$= eV_n \{ -C_{1,n}^{\lambda,p(s)} \exp[-(d_p - z_p)/L_n] + C_{2,n}^{\lambda,p(s)} \exp[(d_p - z_p)/L_n] -$$
$$- A_{1,n}^{\lambda,p(s)} \exp[-\alpha_\lambda (d_p - z_p)] \alpha_\lambda L_n + A_{2,n}^{\lambda,p(s)} \exp[\alpha_\lambda (d_p - z_p)] \alpha_\lambda L_n \}. \quad (29)$$

## 4. Short-circuit current collection from *i*(*n*)-region of a-Si:H layer

Analogous consideration can be made for *i*(*n*)-region of a-Si:H layer (region III), where excess holes contribute mainly to the short-circuit current. In diffusion approximation, Eq. (8) takes the following form in this region:

$$\frac{d^2 \Delta p^{p(s)}}{dz^2} - \frac{\Delta p^{p(s)}}{L_p^2} = -\frac{g^{p(s)}(z)}{D_p}, \quad (30)$$

where $\Delta p^{p(s)}(z) = p^{p(s)}(z) - p_0$. Considering a particular monochromatic component of incident irradiation, the generation function for which is given by the formula (11), a general solution of Eq. (30) analogously to (12) is expressed as

$$\begin{pmatrix} \Delta p_\lambda(z) \\ d\Delta p_\lambda / dz \end{pmatrix}^{p(s)} =$$
$$= C_{1,p}^{\lambda,p(s)} \exp(-z/L_p) \begin{pmatrix} 1 \\ -1/L_p \end{pmatrix} + C_{2,p}^{\lambda,p(s)} \exp(z/L_p) \begin{pmatrix} 1 \\ 1/L_p \end{pmatrix} +$$
$$+ A_{1,p}^{\lambda,p(s)} \exp(-\alpha_\lambda z) \begin{pmatrix} 1 \\ -\alpha_\lambda \end{pmatrix} + A_{2,p}^{\lambda,p(s)} \exp(\alpha_\lambda z) \begin{pmatrix} 1 \\ \alpha_\lambda \end{pmatrix}, \quad (31)$$

where $C_{1,p}^{\lambda,p(s)}$ and $C_{2,p}^{\lambda,p(s)}$ are the coefficients, which has to be determined from the boundary conditions,

$$A_{1,p}^{\lambda,p(s)} = \frac{(1-m)\,\alpha_\lambda\, I_0^{p(s)}(\lambda)\, T_{1\to4}^{p(s)}(\lambda)}{1 - R_{4\to1}^{p(s)}(\lambda)\, R_{4\to5}^{p(s)}(\lambda) \exp[-2\alpha_\lambda (d_p + d + d_n)]} \times$$
$$\times \frac{L_p^2 / D_p}{1 - (\alpha_\lambda L_p)^2},$$
$$A_{2,p}^{\lambda,p(s)} = A_{1,p}^{\lambda,p(s)} R_{4\to5}^{p(s)}(\lambda) \exp[-2\alpha_\lambda (d_p + d + d_n)]. \quad (32)$$

Like to that of electrons, first boundary condition for excess holes can be written in the form of balance equation for hole fluxes at rear a-Si:H surface (interface) (see Fig. 1):

$$-D_p \left. \frac{d\Delta p_\lambda^{p(s)}}{dz} \right|_{z = d_p + d} = S_d\, \Delta p_\lambda^{p(s)}(d_p + d), \quad (33)$$

where $S_d$ is the surface recombination rate for holes. To write the second boundary condition for excess holes at $z = d_p + z_n$, we consider SCR region in the same approximation we have used for electrons in the paragraph 2, i.e. neglecting electron-hole recombination in the SCR layer. In this approximation, Eq. (2) for holes takes the following form:

$$\frac{d i_h^{\lambda,p(s)}}{dz} = g^{p(s)}(z,\lambda), \quad (34)$$

i.e. the flux of excess holes can be written as

$$i_h^{\lambda,p(s)}(z) = i_h^{\lambda,p(s)}(d_p + z_n) +$$
$$+ \tilde{A}_1^{\lambda,p(s)} \exp[-\alpha_\lambda (d_p + z_n)] \{1 - \exp[-\alpha_\lambda (z - d_p - z_n)]\} +$$
$$- \tilde{A}_2^{\lambda,p(s)} \exp[\alpha_\lambda (d_p + z_n)] \{1 - \exp[\alpha_\lambda (z - d_p - z_n)]\}, \quad (35)$$

where coefficients $\tilde{A}_1^{\lambda,p(s)}$ and $\tilde{A}_2^{\lambda,p(s)}$ are given by the formulae (23) and (24), respectively. Relation between the hole flux $i_h^{\lambda,p(s)}$ and the hole concentration is given by Eq. (6), which in 1D case can be rewritten as:

$$\frac{dp_\lambda^{p(s)}}{dz} + p_\lambda^{p(s)} \frac{dy}{dz} = -\frac{i_h^{\lambda,p(s)}}{D_p}. \quad (36)$$

Similarly to the case of electrons, at equilibrium, when $i_h^{\lambda,p(s)} = 0$, solution of the latter equation has the following form:

$$p_\lambda^{p(s)}(z) \equiv p_0(z) = p_p \exp[-y(z) - y_{pn}], \quad (37)$$

where $p_p$ is the hole concentration in $p^+$-region beyond the SCR layer, where holes are the majority carriers. In the case of irradiation, when $i_h^{\lambda,p(s)} \neq 0$, the solution of Eq. (36) can be found in the form

$$p_\lambda^{p(s)}(z) = B_p^{\lambda,p(s)}(z) \exp[-y(z)], \quad (38)$$

where the pre-exponential function $B_p^{\lambda,p(s)}(x)$ is a solution of the following differential equation:

$$\frac{dB_p^{\lambda,p(s)}}{dz} = -\exp[y(z)]\, i_h^{\lambda,p(s)}(z) / D_p. \quad (39)$$

A general solution of this equation can be written as

$$B_p^{\lambda,p(s)}(z) = B_{p0} - \frac{1}{D_p} \int_{z_0}^{z} \exp[y(z')] i_h^{\lambda,p(s)}(z')\, dz', \quad (40)$$

where $B_{p0}$ and $x_0$ are two arbitrary constants. Substituting (40) into (38), we obtain following expression for $p_\lambda^{p(s)}(z)$ in the SCR region:

$$p_\lambda^{p(s)}(z) =$$
$$= \exp[-y(z)] \left\{ p_p \exp(-y_{pn}) - \frac{1}{D_p} \int_{d_p - z_p}^{z} \exp[y(z')]\, i_h^{\lambda,p(s)}(z')\, dz' \right\}, \quad (41)$$

© 2012, V. Lashkaryov Institute of Semiconductor Physics, National Academy of Sciences of Ukraine

where values of $B_{p0}$ and $z_0$ are chosen to provide right $p_\lambda^{p(s)}(z) = p_p$ value at $z = d_p - z_p$ (no accumulation of excess holes is supposed in a-Si:H $p^+$-region beyond the SCR layer at short-circuit current conditions, i.e. all the holes supplied by $i(n)$-region to $p^+$-region and generated in $p^+$-region pass away to the front surface contact or recombine with electrons, so that the hole concentration in this region remains practically equilibrium.

Thus, as it follows from Eq. (41),

$$p_\lambda^{p(s)}(d_p + z_n) - p_p \exp(-y_{pn}) \equiv \Delta p_\lambda^{p(s)}(d_p + z_n) = -\frac{1}{D_p} \int_{d_p - z_p}^{d_p + z_n} \exp[y(z)]\, i_h^{\lambda,p(s)}(z)\, dz. \quad (42)$$

According to (6), the flux $i_h^{\lambda,p(s)}$ at the SCR boundary $z = d_p + z_n$ in Eq. (35) can be expressed as

$$i_h^{\lambda,p(s)}(d_p + z_n) = -D_p \left.\frac{d\Delta p_\lambda^{p(s)}}{dz}\right|_{z = d_p + z_n}, \quad (43)$$

so that two boundary conditions (33) and (42) can be rewritten in the form of the following two explicit algebraic equations for the coefficients $C_{1,p}^{\lambda,p(s)}$ and $C_{2,p}^{\lambda,p(s)}$:

$$\begin{aligned} &C_{1,p}^{\lambda,p(s)} \exp[-(d_p + d)/L_p](S_d - V_p) + \\ &+ C_{2,p}^{\lambda,p(s)} \exp[(d_p + d)/L_p](S_d + V_p) = \\ &= A_{1,p}^{\lambda,p(s)} \exp[-\alpha_\lambda (d_p + d)](V_p \alpha_\lambda L_p - S_d) - \\ &- A_{2,p}^{\lambda,p(s)} \exp[\alpha_\lambda (d_p + d)](V_p \alpha_\lambda L_p + S_d), \end{aligned} \quad (44)$$

$$\begin{aligned} &C_{1,p}^{\lambda,p(s)} \exp[-(d_p + z_n)/L_p]\,(1 + I_{y+}) + \\ &+ C_{2,p}^{\lambda,p(s)} \exp[(d_p + z_n)/L_p]\,(1 - I_{y+}) = \\ &= A_{1,p}^{\lambda,p(s)} \left\{ -\exp[-\alpha_\lambda (d_p + z_n)] \left[ \frac{I_{y+}}{\alpha_\lambda L_p} + 1 \right] + \frac{1 - (\alpha_\lambda L_p)^2}{\alpha_\lambda L_p} I_{y+}^{\alpha_\lambda -} \right\} + \\ &+ A_{2,p}^{\lambda,p(s)} \left\{ \exp[\alpha_\lambda (d_p + z_n)] \left[ \frac{I_{y+}}{\alpha_\lambda L_p} - 1 \right] - \frac{1 - (\alpha_\lambda L_p)^2}{\alpha_\lambda L_p} I_{y+}^{\alpha_\lambda +} \right\}, \end{aligned} \quad (45)$$

where $V_p = D_p / L_p$, $I_{y+} = \int_{d_p - z_p}^{d_p + z_n} \exp[y(z)]\, dz / L_p$,

$$I_{y+}^{\alpha -} = \int_{d_p - z_p}^{d_p + z_n} \exp[y(z) - \alpha z]\, dz / L_p,$$

$$I_{y+}^{\alpha +} = \int_{d_p - z_p}^{d_p + z_n} \exp[y(z) + \alpha z]\, dz / L_p.$$

Calculating coefficients $C_{1,p}^{\lambda,p(s)}$ and $C_{2,p}^{\lambda,p(s)}$ from the system of algebraic equations (44) and (45), we completely determine the hole component of the density of short-circuit current $j_{h,SC}^{\lambda,p(s)}$:

$$\begin{aligned} &j_{h,SC}^{\lambda,p(s)} \equiv e i_h^{\lambda,p(s)}(d_p + z_n) = \\ &= eV_p \Big\{ C_{1,p}^{\lambda,p(s)} \exp[-(d_p + z_n)/L_p] - C_{2,p}^{\lambda,p(s)} \exp[(d_p + z_n)/L_p] + \\ &+ A_{1,p}^{\lambda,p(s)} \exp[-\alpha_\lambda (d_p + z_n)]\, \alpha_\lambda L_p - A_{2,p}^{\lambda,p(s)} \exp[\alpha_\lambda (d_p + z_n)]\, \alpha_\lambda L_p \Big\}. \end{aligned} \quad (46)$$

## 5. Calculation of DOS and position of Fermi-level in a-Si:H

In the first approximation, the dependence $y(x)$ in SCR at short-circuit current conditions is close to the equilibrium one, which is realized in dark, when no excess carriers are produced by irradiation in the a-Si:H layer. To calculate $y(x)$ in SCR, first of all we have to determine the energy position of Fermi levels in $p^+$- and $i(n)$-regions of a-Si:H layer beyond SCR (i.e. in regions I and II). In amorphous silicon a large number of energy levels in the band gap exists even without special doping of material. These levels have different origin and influence substantially the position of Fermi energy level in intrinsic material. They are formed by three main groups of states. The first group is presented by weak-bond valence-band-tail states of the donor-like type. If the valence band apex is taken as zero energy level, then the energy distribution of the one-electron states in this group can be approximately described by the following formula:

$$N_{vt}(E,T) = N_{vt0} \exp(-E / E_{v0}), \quad (47)$$

where $N_{vt0} = (1...3)\cdot 10^{21}\ \text{cm}^{-3}\,\text{eV}^{-1}$ (see, e.g. [1-3]), although in the literature larger values up to $N_{vt0} \approx 7\cdot 10^{21}\ \text{cm}^{-3}\,\text{eV}^{-1}$ also can be found (see, e.g. [4, 5]), the characteristic energy $E_{v0}$ is a function of temperature, $E_{v0}(T) = \sqrt{E_{v0}^2(T^*) - (kT^*)^2 + (kT)^2}$, $T^* = 500$ K is the equilibration temperature [1, 2]. Depending on the quality of a-Si:H material, $E_{v0}$ can vary from 0.04 up to 0.15 eV at $T = 300$ K. In our calculations, the value $E_{v0}(T^*) = 0.056$ eV has been used as a parameter to which the value $E_{v0}(300\ \text{K}) =$ 0.045 eV corresponds.

Another group of energy levels in the band gap of a-Si:H material is formed by conduction-band-tail acceptor-like states, energy distribution of which can be approximately described by the analogous formula:

$$N_{ct}(E) = N_{ct0} \exp[(E - E_g)/E_{c0})], \quad (48)$$

where $N_{ct0}$ varies within the range from $10^{21}$ to $10^{22}\ \text{cm}^{-3}\,\text{eV}^{-1}$ [1–5].

Besides, dangling bond defects exist in a-Si:H material, which form deep defect states in the a-Si:H band gap [1, 2]. The density of these states is dependent on the position of the Fermi level in the band gap due to specific microscopic reactions involving hydrogen [1, 2].

*© 2012, V. Lashkaryov Institute of Semiconductor Physics, National Academy of Sciences of Ukraine*

These microscopic reactions lead to formation of deep defect states from weak-bond band-tail states (47). As it follows from the formulae (20) and (25) of the work [2], the contribution $dD_t(E)$ into the density of deep defect states at an energy $E$ from the weak bond states (47) with the energies within the range $dE_t$ in the vicinity of $E_t$ can be expressed at temperatures $T > T^*$ as

$$dD(E, E_t, T) = \\ = \frac{N_{vt}(E_t)\, dE_t\, P(E)}{1+\exp\{[E+(kT/2)\ln(N_{\mathrm{SiSi}}/N_{\mathrm{H}})-2E_t]/kT\}}, \quad (49)$$

where $N_{\mathrm{SiSi}}$ is approximately equal to $2\cdot 10^{23}\ \mathrm{cm}^{-3}$ and defines the total number of electrons in silicon bonding states (four electrons per Si atom), $N_{\mathrm{H}}$ is the total concentration of hydrogen in a-Si:H material ($N_{\mathrm{H}}$ is close to $5\cdot 10^{21}\ \mathrm{cm}^{-3}$ at hydrogen content [H] = 10 at.%), $P(E)$ is the defect-pool function (normalized to the unity energy distribution function of potential defect sites in a-Si:H material, from which deep defect states can be formed with the energy $E$), $P(E)$ is usually taken as Gaussian:

$$P(E) = (2\pi\sigma^2)^{-1/2} \exp[-(E-E_p)^2/(2\sigma^2)], \quad (50)$$

where $\sigma$ is the pool width and $E_p$ is the most probable potential defect energy. According to Powell and Deane [1, 2], $\sigma$ can be determined from the experimentally measured energy separation $\Delta = 0.44$ eV between the doubly occupied defect state and empty defect one; $\sigma = [E_{v0}(T)\cdot(\Delta+U)]^{1/2}$, where $U = 0.2...0.3$ eV is the defect electron correlation energy accounting for electron interaction in negatively charged defects, when the second electron is placed on the defect; $E_p = 1.27$ eV in material with the band gap $E_g = 1.9$ eV. As the band gap depends on the hydrogen content in a-Si:H, in our calculations we have used the value $E_p = (E_g/1.9\,\mathrm{eV})\cdot 1.27\,\mathrm{eV}$. For $E_g([\mathrm{H}])$-dependence, we have used the linear approximation $E_g$ = (1.58 + 0.017 [H]) eV, which corresponds to the data of the work [6]. In practice, the coefficient before the hydrogen content [H] can vary from 0.012 up to 0.025 depending on a-Si:H material quality. The total density of dangling bond states is thus expressed as

$$D(E,T) = \int_0^{E_g} \frac{N_{vt}(E_t)\, dE_t\, P(E)}{1+\exp\{[E+(kT/2)\ln(N_{\mathrm{SiSi}}/N_{\mathrm{H}})-2E_t]/kT\}}. \quad (51)$$

This density of states includes contributions from neutral, positively and negatively charged defects. If charged defects are accounted in the law of mass action equations, then, following [2], it is necessary to replace the defect energy $E$ in the integrand in the right-hand side of Eq. (51) with the defect chemical potential $\mu_d = E + kT\ln[f^0(E)/2]$, where $f^0(E)$ is the neutral defect occupation function for amphoteric silicon dangling bonds:

$$f^0(E) = \frac{2\exp[(E_F-E)/kT]}{1+2\exp[(E_F-E)/kT]+\exp[(2E_F-2E-U)/kT]}. \quad (52)$$

As a result, the density of dangling bond states becomes dependent on the position of the Fermi energy $E_F$ in a-Si:H material. Performing integration in (51), the following expression for $D(E,T)$ has been obtained in [2] for this case:

$$\tilde{D}(E, E_F, T) = \gamma \left[\frac{2}{f^0(E)}\right]^{kT/2E_{v0}} P\left(E + \frac{\sigma^2}{2E_{v0}}\right), \quad (53)$$

where

$$\gamma = N_{v0}\left(\frac{N_{\mathrm{H}}}{N_{\mathrm{SiSi}}}\right)^{kT/4E_{v0}} \left(\frac{2E_{v0}^2}{2E_{v0}-kT}\right) \exp\left[-\frac{1}{2E_{v0}}\left(E_p - \frac{\sigma^2}{4E_{v0}}\right)\right]. \quad (54)$$

All three types of defects can be donor-like, characterized by one-electron transitions of the type (+/0), and acceptor-like, characterized by one-electron transitions of the type $(-/0)$. In accordance with [2], the density of one-electron acceptor-like states is expressed as

$$g_A(E, E_F, T) = \tilde{D}(E + kT\ln 2, E_F, T), \quad (55)$$

while that of donor-like as

$$g_D(E, E_F, T) = \tilde{D}(E - U - kT\ln 2, E_F, T). \quad (56)$$

At temperatures $T < T^*$, the densities of defect states do not depend on temperature. During cooling the grown material below $T^*$, they leave "frozen-in", i.e. $\tilde{D}(E, E_F, T < T^*) = \tilde{D}(E, E_F^*, T^*)$, where $E_F^*$ is the Fermi energy calculated at equilibrium temperature $T^*$. Remember that the valence-band-tail characteristic energy $E_{v0}$, as pointed earlier, is also a function of temperature, i.e. the value $E_{v0}(T^*) = 0.056$ eV has to be used at $\tilde{D}(E, E_F, T < T^*)$ calculations.

Due to participation of the valence band-tail states in deep defect states formation, their density of states becomes depleted, i.e. instead of $N_{vt}(E)$ in formula (47), a depleted density of states

$$\tilde{N}_{vt}(E_t, T) = \\ = N_{vt}(E_t, T)\left\{1 - \int_0^{E_g} \frac{P(E)\, dE}{1+(N_{\mathrm{SiSi}}/N_{\mathrm{H}})^{1/2}\exp[(E-2E_t)/kT]}\right\} \quad (57)$$

has to be used in calculations at $T > T^*$ and

$$\tilde{N}_{vt}(E_t, T) = N_{vt}(E_t, T) - \\ -N_{vt}(E_t, T^*)\int_0^{E_g} \frac{P(E)\, dE}{1+(N_{\mathrm{SiSi}}/N_{\mathrm{H}})^{1/2}\exp[(E-2E_t)/kT^*]}, \quad (58)$$

*© 2012, V. Lashkaryov Institute of Semiconductor Physics, National Academy of Sciences of Ukraine*

if $\tilde{N}_{vt}(E_t,T) > 0$ or $\tilde{N}_{vt}(E_t,T) = 0$ and if the expression in the right-hand side of the formula (58) becomes lower than zero at $T < T^*$.

In addition to above states always present in intrinsic a-Si:H, the donor and acceptor states introduced by special doping a-Si:H material have to be accounted. If doping of a-Si:H with donors is made (e.g. by phosphorous), the density of donor states often can be characterized by the normal Gaussian distribution of the states on their energy:

$$N_D(E,z) = N_{D0}(z)\frac{1}{\sigma_D\sqrt{2\pi}}\exp\left[-\frac{(E-E_g+E_D)^2}{2\sigma_D^2}\right], \quad (59)$$

where $N_{D0}$ is the concentration of donor states, $\sigma_D$ is the energy width of the distribution, and $E_D$ is the donor ionization energy in the maximum of the distribution (59).

Analogous Gaussian distribution can be introduced to describe acceptor density of states in the band gap (e.g., when doping a-Si:H with boron atoms is made):

$$N_A(E,z) = N_{A0}(z)\frac{1}{\sigma_A\sqrt{2\pi}}\exp\left[-\frac{(E-E_A)^2}{2\sigma_A^2}\right], \quad (60)$$

where $N_{A0}$ is the concentration of acceptor states, $\sigma_A$ – energy width of the acceptor states distribution, and $E_A$ – acceptor ionization energy in the maximum of the distribution (60). $N_{D0}$ and $N_{A0}$ are constants in $i(n)$- and $p^+$-regions, respectively, and change to zero at $p^+-i(n)$ junction. In the case of ideal $p^+-i(n)$ junction, these changes have a step-like character, i.e. $N_{A0}$ and $N_{D0}$ turn to zero exactly at $z = d_p$. However, if $p^+-i(n)$ junction is somewhat degraded (e.g., due to diffusion of acceptors or/and donors after junction formation, or due to pure technological reasons at $p^+-i(n)$ junction growth) they become coordinate dependent functions in a thin transition layer at $z = d_p$. To account for possible $p^+-i(n)$ junction degradation, we use the following coordinate dependent functions $N_{A0}$ and $N_{D0}$ in our subsequent calculations of band bending:

$$N_{A0}(z) = \frac{n_A}{2}\left[1-\mathrm{erf}\left(\frac{z-d_p}{\sigma'_A\sqrt{2}}\right)\right], \quad (61)$$

and

$$N_{D0}(z) = \frac{n_D}{2}\left[1+\mathrm{erf}\left(\frac{z-d_p}{\sigma'_D\sqrt{2}}\right)\right], \quad (62)$$

where $n_A$ and $n_D$ are the concentrations of acceptor and donors far from degraded region in $p^+$- and $n$- parts of a-Si:H (if $i$-region is doped additionally by donors), $\sigma'_A$ and $\sigma'_D$ are the width of degraded regions at $p^+-i(n)$ junction for acceptors and donors, respectively, erf($z$) is the "error function":

$$\mathrm{erf}(z) = \frac{2}{\sqrt{\pi}}\int_0^z \exp(-t^2)\,dt\,. \quad (63)$$

At distances $|z-d_p| \geq \sigma'_A, \sigma'_D$

$$N_D(E,z) \equiv \tilde{N}_D(E) = \frac{n_D}{\sigma_D\sqrt{2\pi}}\exp\left[-\frac{(E-E_g+E_D)^2}{2\sigma_D^2}\right], \quad (64)$$

$$N_A(E,z) \equiv \tilde{N}_A(E) = \frac{n_A}{\sigma_A\sqrt{2\pi}}\exp\left[-\frac{(E-E_A)^2}{2\sigma_A^2}\right]. \quad (65)$$

Fig 2 demonstrates introduced coordinate dependences (61) and (62) of acceptor and donor concentrations $N_{A0}$ and $N_{D0}$ in thin transition technological layer at $p^+-i(n)$ junction.

Finally, to write the charge balance equation, from which the Fermi energy $E_F$ can be found, we have to connect correctly (i.e. smoothly and continuously) conduction and valence band-tail densities of states with the densities of free electron and hole states in conduction and valence bands, respectively. Conduction band density of states is expressed in a-Si:H as

$$N_c(E) = N_{c0}\,(E-E_g)^{1/2}, \quad (66)$$

where

$$N_{c0} = \frac{1}{2\pi^2}\left(\frac{2m_e}{\hbar^2}\right)^{3/2} = 6.791\cdot10^{21}\left(\frac{m_e}{m_0}\right)^{3/2}\ \mathrm{cm^{-3}\cdot eV^{-3/2}}, \quad (67)$$

Analogously, the valence band density of states is expressed as

$$N_v(E) = N_{v0}\,(-E)^{1/2}, \quad (68)$$

where $N_{v0}$, like to $N_{c0}$, is expressed by the formula (67) with the only difference that instead of electron effective mass $m_e$ hole effective mass $m_h$ has to be substituted to this formula, $m_0$ is the free electron mass.

To connect densities of states in conduction and valence bands (66) and (68) with band-tail densities of states (48) and (47), we have to find energies, at which smooth and continuous relation can be made. At these energies

$$N_c(E) = N_{ct}(E), \quad (69)$$

$$\frac{dN_c}{dE} = \frac{dN_{ct}}{dE}. \quad (70)$$

$$N_v(E) = N_{vt}(E), \quad (71)$$

$$\frac{dN_v}{dE} = \frac{dN_{vt}}{dE}. \quad (72)$$

Like to that in the work [4], from the system of the equations (69) and (70) the corresponding energy

© 2012, V. Lashkaryov Institute of Semiconductor Physics, National Academy of Sciences of Ukraine

$E_c = E_g + E_{c0}/2$ can be found, which practically coincides with the energy of conduction band bottom. The energy $E_v = -E_{v0}/2$, practically coinciding with the valence band apex, is analogous to the energy in the equations (71) and (72).

To satisfy Eqs. (69)-(72) for physically correct values $10^{21}...10^{22}\,\text{cm}^{-3}\text{eV}^{-1}$ of the band-tail densities of states $N_{vt0}$ and $N_{ct0}$, it turns out that larger effective masses of electrons and holes has to be used, than $m_e$ close to $m_0$ and $m_h = 0.5m_0$ presented in many publications on a-Si:H material. We have used in our work the values $m_e = 2.78m_0$ and $m_h = 2.34m_0$ from the recent publication [7]. It is these effective masses that the values $N_{ct0} = 2.1\times10^{21}\,\text{cm}^{-3}\text{eV}^{-1}$ and $N_{vt0} = 2.2\times10^{21}\,\text{cm}^{-3}\text{eV}^{-1}$ correspond to.

In Fig. 3, the calculated densities of states in the band gap are shown, which are continuously and smoothly related with the densities of free charge states in conduction and valence bands.

The concentration $n_c$ of free electrons in the conduction band for the Fermi level lying inside the band gap is expressed as

$$n_c(E_F,T) = \nu_c \exp\left(\frac{E_F - E_g}{kT}\right), \tag{73}$$

where $\nu_c$ is the effective density of states at the conduction band bottom

$$\nu_c = \frac{2}{\hbar^3}\left(\frac{m_e kT}{2\pi}\right)^{3/2} \approx 2.5\cdot10^{19}\left(\frac{m_e}{m_0}\right)^{3/2}\left(\frac{T}{300\,K}\right)^{3/2}\text{cm}^{-3}. \tag{74}$$

As to free holes in the valence band, their concentration is expressed by the analogous formula:

$$n_v(E_F,T) = \nu_v \exp\left(-\frac{E_F}{kT}\right), \tag{75}$$

where

$$\nu_v = \frac{2}{\hbar^3}\left(\frac{m_h kT}{2\pi}\right)^{3/2} \approx 2.5\cdot10^{19}\left(\frac{m_h}{m_0}\right)^{3/2}\left(\frac{T}{300\,K}\right)^{3/2}\text{cm}^{-3}. \tag{76}$$

Now it is possible to write the charge balance equation:

$$n_c(E_F,T) + \int_0^{E_g} \frac{N_{ct}(E) + \tilde{N}_A(E) + g_A(E,E_F,T)}{1 + 2\exp[(E - E_F)/kT]}\,dE = n_v(E_F,T) + \int_0^{E_g} \frac{\tilde{N}_{vt}(E,T) + \tilde{N}_D(E) + g_D(E,E_F,T)}{1 + 2\exp[(E_F - E)/kT]}\,dE, \tag{77}$$

where in the left hand side of the equation the negative charge of free electrons in conduction band and of electrons captured by acceptor and acceptor-like states inside band gap is written, while in the right hand side – the positive charge of free holes in the valence band and holes captured by donor and donor-like states. The degeneracy coefficient 2 at the exponents in the denominators of integrand expression accounts for right statistics of the localized band gap states.

To calculate Fermi levels in $p^+$- and $i(n)$-regions of a-Si:H layer at $T$ = 300 K, it is necessary to determine previously from Eq. (77) the Fermi levels at the equilibrium temperature $T^*$ = 500 K to find the "frozen-in" densities of states of dangling bond defects $g_A(E,E_F^*,T^*)$ and $g_D(E,E_F^*,T^*)$, and then again solve Eq. (77) at $T$ = 300 K, but with $g_A(E,E_F^*,T^*)$ and $g_D(E,E_F^*,T^*)$ densities instead of $g_A(E,E_F,T)$ and $g_D(E,E_F,T)$. The value of Fermi energy 1.05 eV has been found from Eq. (77) both at $T$ = 300 K and $T^*$ = 500 K in intrinsic a-Si:H, when no special doping is made. In doped a-Si:H, the values of Fermi energy at $T$ = 300 K and $T^*$ = 500 K can differ remarkably, depending on the doping level $n_A$ ($n_D$).

## 6. Band bending in space charge region at $p^+$-$i(n)$ junction in a-Si:H layer

After calculating the Fermi levels $E_F^P$ and $E_F^{i(n)}$ in equilibrium conditions in $p^+$- and $i(n)$-regions of a-Si:H layer, respectively, we can determine the total band bending $y_{np}$ (see Eq. 25) at $p^+ - i(n)$ junction:

$$y_{pn} = (E_F^{i(n)} - E_F^P)/kT. \tag{78}$$

To find the shape of band bending $y(z)$ in SCR in equilibrium conditions (when irradiation is absent) the corresponding Poisson equation has to be solved for the electrostatic potential. Rewritten in the form of equation for $y(x)$ this equation takes up the following form (Gaussian CGS system of units is used):

$$\frac{d^2y}{dz^2} = \frac{4\pi e^2}{\varepsilon kT}\times \left\{\nu_c \exp\left[\frac{E_F^{i(n)} - E_g}{kT} + y(z,T)\right] - \nu_v \exp\left[-\frac{E_F^{i(n)}}{kT} - y(z,T)\right] + \int_0^{E_g} \frac{N_{ct}(E) + N_A(E,z) + g_A(E,E_F^{i(n)} + kT\,y(z,T),T)}{1 + 2\exp[(E - E_F^{i(n)})/kT - y(z,T)]}\,dE - \int_0^{E_g} \frac{\tilde{N}_{vt}(E,T) + N_D(E,z) + g_D(E,E_F^{i(n)} + kT\,y(z,T),T)}{1 + 2\exp[(E_F^{i(n)} - E)/kT + y(z,T)]}\,dE\right\}, \tag{79}$$

where ε is static dielectric permittivity of a-Si:H material. A solution of this equation has to satisfy two boundary conditions. At SCR boundary in $i(n)$-region of a-Si:H, it has tend to zero, while at another SCR

© 2012, V. Lashkaryov Institute of Semiconductor Physics, National Academy of Sciences of Ukraine

boundary in $p^+$-region to $-y_{pn}$. To solve numerically Eq. (79) and to determine the position of SCR boundaries, we consider $p^+$- and $i(n)$-regions of a-Si:H as being thick enough not to account for the influence of other junctions. Then, by calculating $y(z,T)$ it becomes convenient to use new coordinate $z' = z - d_p$. In the new coordinate system starting points $z''$ for Eq. (79) numerical solution have to be located in the vicinity of $z' = 0$. These starting points can differ from $z' = 0$ due to account of possible $p^+ - i(n)$ junction degradation (see Fig. 2). By numerical solution of Eq. (79), it is necessary to assign starting values to $y$ and $dy/dz'$ at $z' = z''$. Value $y(z'',T)$ is directly and unambiguously determined from the right-hand side of Eq. (79): $y(z'',T)$ is the value, at which right-hand side of Eq. (79) (i.e. local charge) turns to zero. Concerning the derivative $dy/dz'$ at the starting point $z''$ and the starting point $z''$ itself, they are considered as parameters, allowing to satisfy above mentioned boundary conditions at SCR boundaries. By change of $z''$, the starting value of the derivative $(dy/dz')_+$ at this point for Eq. (79) numerical solution in $i(n)$-region ($z' > 0$), and starting value of the derivative $(dy/dz')_-$ for Eq. (79) numerical solution in $p^+$-region ($z' < 0$), we find such point $z''$, for which not only both boundary conditions at SCR boundary are satisfied, but the difference $(dy/dz')_+ - (dy/dz')_-$ tends to zero, too, i.e. smooth and continuous band bending is achieved at $p^+ - i(n)$ junction. The equality $(dy/dz')_+ = (dy/dz')_-$ at $z' = z''$ expresses the condition of total neutrality of SCR, i.e. that a positive charge in the SCR at $z' > z''$ is completely compensated by a negative charge at $z' < z''$.

Cutting off the tail of the calculated $y(z)$-dependence in $i(n)$-region, which is smaller by its absolute value than unity (i.e. cutting off the physically unresonable potential energies $|e\varphi| < kT$), we find thus the physical thickness $z_n$ of the SCR in $i(n)$-part of a-Si:H. Analogously, cutting off the physically unresonable tail of the calculated $y(z)$-dependence in $p^+$-region, which differs from $-y_{pn}$ by the value less than unity, we find the physical thickness $z_p$ of the SCR in $p^+$-part of a-Si:H.

Analogously to the Fermi energy calculation, to obtain the band bending $y(z',T)$ at $T < T^*$ it is necessary first to calculate band bending $y(z',T^*)$ by solving the differential equation (79) at the equilibrium temperature $T^* = 500\,\mathrm{K}$. Thus, the local distributions of dangling bond defects $g_A(E, E_F^{i(n)*} + kT^* y(z',T^*), T^*)$ and $g_D(E, E_F^{i(n)*} + kT^* y(z',T^*), T^*)$ for every local position of the Fermi level $E_F^{i(n)*} + kT^* y(z',T^*)$ relatively to the valence band apex can be determined at every point $z'$ of SCR. These "frozen-in" distributions have to be substituted into Eq. (79) instead of $g_A(E, E_F^{i(n)} + kT\, y(z',T), T)$ and $g_D(E, E_F^{i(n)} + kT\, y(z',T), T)$ by subsequent calculation of band bending $y(z',T)$ at $T < T^*$.

Fig. 4 demonstrates the calculated band bending in a-Si:H for several types of doping.

Figs. 5 and 6 demonstrate the calculated bending of conduction band (upper curves) and valence band (lower curves) at $p^+ - i(n)$ junction in a-Si:H for material with the band gap $E_g$ = 1.75 eV (10% hydrogen content).

With the found band bending shape $y(z)$ and determined thicknesses $z_n$ of SCR in $i(n)$-region and $z_p$ in $p$-region, all the integrals in Eqs. (28) and (45) can be easily calculated.

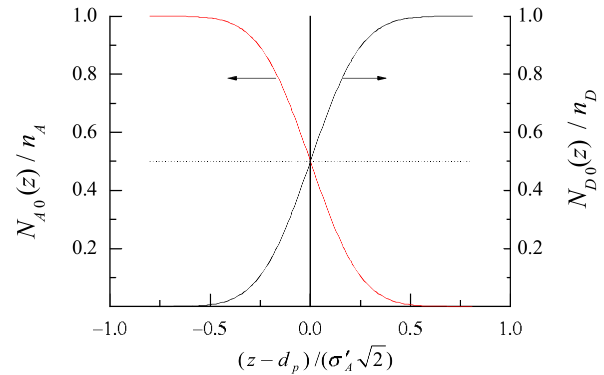


**Fig. 2.** Used model of degraded $p^+$-$i(n)$ junction in a-Si:H.

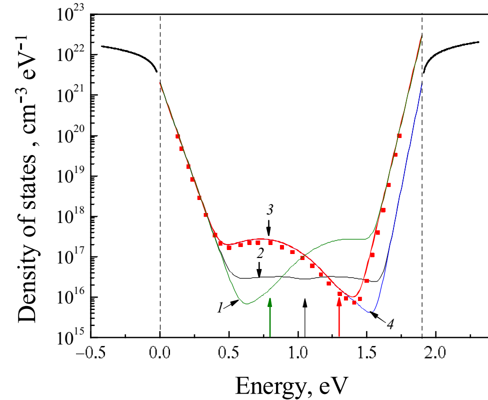


**Fig. 3.** Density of states in a-Si:H for various positions of the Fermi level in the case of a-Si:H material with the band gap 1.9 eV. Common parameters for all the curves: $E_{v0}$ = 45 meV, $N_{vt0}$ = 2 × $10^{21}$ cm$^{-3}$eV$^{-1}$. Dashed vertical lines mark the valence band apex (left line) and the conduction band bottom (right line). Vertical arrows at energies 0.8, 1.05 and 1.3 eV mark three different positions of the Fermi level, for which calculations have been fulfilled. Dots show the density of states in the band gap, which has been calculated in [2] for the Fermi energy position at 1.3 eV. Parameters of the curve *1*: $E_F$=0.8 eV, $E_{ct0}$ = 30 meV, $N_{ct0}$ = 3 × $10^{22}$ cm$^{-3}$eV$^{-1}$; curve *2*: $E_F$ = 1.05 eV, $E_{ct0}$ = 25 meV, $N_{ct0}$ = 2 × $10^{21}$ cm$^{-3}$eV$^{-1}$; curve *3*: $E_F$=1.3 eV, $E_{ct0}$ = 30 meV, $N_{ct0}$ = 3 × $10^{22}$ cm$^{-3}$eV$^{-1}$; curve *4*: $E_F$ = 1.3 eV, $E_{ct0}$ = 25 meV, $N_{ct0}$ = 2 × $10^{21}$ cm$^{-3}$eV$^{-1}$.

*© 2012, V. Lashkaryov Institute of Semiconductor Physics, National Academy of Sciences of Ukraine*

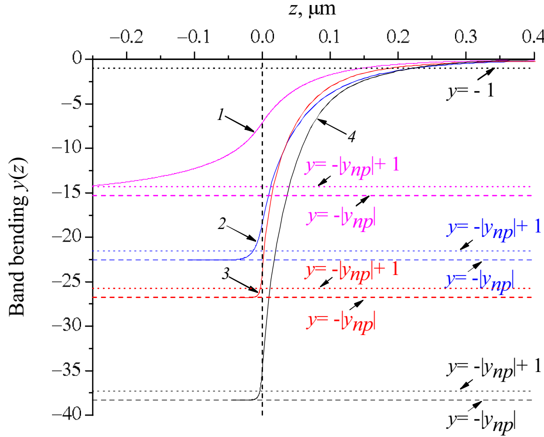


**Fig. 4.** Calculated shapes of band bending at $T$ = 300 K at $p^+ - i(n)$ junction in a-Si:H. Parameters of acceptor and donor distributions: $E_A$ = 0.2 eV, $\sigma_A$ = 0.1 eV, $\sigma'_A = 0.5$ nm, $E_D$ = 0.3 eV, $\sigma_D$ = 0.1 eV, $\sigma'_D = 0.5$ nm. Curve *1*: $n_A = 10^{17}$ cm$^{-3}$, $n_D$ = 0; curve *2*: $n_A = 10^{18}$ cm$^{-3}$, $n_D$ = 0; curve *3*: $n_A = 10^{19}$ cm$^{-3}$, $n_D$ = 0; curve *4*: $n_A = 10^{19}$ cm$^{-3}$, $n_D = 10^{17}$ cm$^{-3}$.

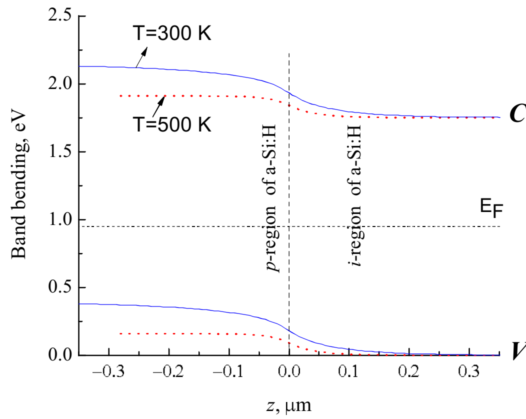


**Fig. 5.** Calculated conduction ($C$) and valence ($V$) band bending at $p^+ - i(n)$ junction in a-Si:H at $T$ = 300 K and $T$ = 500 K. Parameters of acceptor distribution in *p*-region: $E_A$ = 0.2 eV, $\sigma_A$ = 0.1 eV, $\sigma'_A = 0.5$ nm, $n_A = 10^{17}$ cm$^{-3}$. No doping of *i*-region is made, $n_D$ = 0.

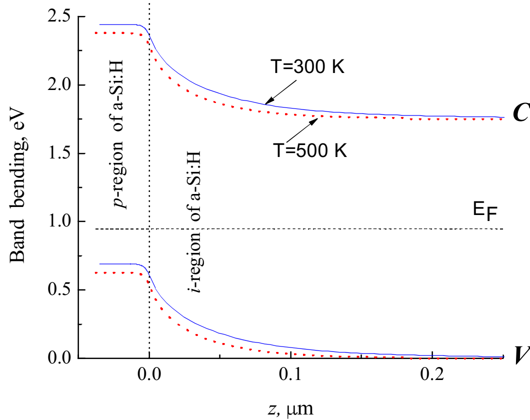


**Fig. 6.** Same as in Fig. 5, but for doping level of *p*-region $n_A = 10^{19}$ cm$^{-3}$.

## 7. Light transmission and reflection in the SC structure

As known from electrodynamics, for electric and magnetic field strengths $\boldsymbol{E}_j$ and $\boldsymbol{H}_j$ in the monochromatic electromagnetic waves, spreading in the material with the index $j$ ($j = 1...5$, see Fig. 1), the following wave equations can be written:

$$\nabla^2 \boldsymbol{E}_j + \frac{\omega^2}{c^2}\varepsilon_j(\omega)\boldsymbol{E}_j = 0 \,, \tag{80}$$

$$\nabla^2 \boldsymbol{H}_j + \frac{\omega^2}{c^2}\varepsilon_j(\omega)\boldsymbol{H}_j = 0 \,, \tag{81}$$

where $\varepsilon_j(\omega) = \varepsilon'_j(\omega) + i\varepsilon''_j(\omega)$ is the dielectric permittivity of the *j*-material, $\varepsilon'_j(\omega)$ and $\varepsilon''_j(\omega)$ are real and imaginary parts of the permittivity, $c$ is the light velocity in vacuum, $\omega$ is the frequency, $\omega = 2\pi c/\lambda$, where $\lambda$ is the wavelength. For the incident onto SC irradiation is a package of monochromatic plane waves, the solutions of Eqs. (80) and (81) inside SC can be represented as plane waves, too:

$$\boldsymbol{E}_j = \boldsymbol{E}^+_{oj}\exp(i\boldsymbol{k}^+_j\boldsymbol{r}) + \boldsymbol{E}^-_{oj}\exp(i\boldsymbol{k}^-_j\boldsymbol{r}) \,, \tag{82}$$

$$\boldsymbol{H}_j = \boldsymbol{H}^+_{oj}\exp(i\boldsymbol{k}^+_j\boldsymbol{r}) + \boldsymbol{H}^-_{oj}\exp(i\boldsymbol{k}^-_j\boldsymbol{r}) \,, \tag{83}$$

where $\boldsymbol{k}^{+(-)}_j$ are the wave vectors, squares of which are expressed as

$$[k^{+(-)}_j]^2 = \frac{\omega^2}{c^2}[\varepsilon'_j(\omega) + i\varepsilon''_j(\omega)] \,. \tag{84}$$

As it follows from the boundary conditions at front surface and interfaces inside the structure, in a general case of oblique incidence of monochromatic electromagnetic plane waves onto the front surface of SC, the *x*-component of the wave vectors (in the plane of incidence) for all electromagnetic waves in all SC layers has to be the same as that in vacuum (air), i. e. $k^{+(-)}_{x,j} = k_x = (\omega/c)\sin\theta$, where $\theta$ is the angle of incidence (angle between directions of SC growth and electromagnetic wave propagation in vacuum). Thus, for *z*-components of electromagnetic waves in the structure the following expression is valid:

$$k^{+(-)}_{z,j} = \pm k_{z,j} \,, \tag{85}$$

where

$$k_{z,j} = \sqrt{\frac{\omega^2}{c^2}\left[\varepsilon'_j(\omega) + i\varepsilon''_j(\omega)\right] - \frac{\omega^2}{c^2}\sin^2\theta} = \frac{\omega}{c}\left[n_{z,j}(\omega,\theta) + i\kappa_{z,j}(\omega,\theta)\right], \tag{86}$$

$$n_{z,j}(\omega,\theta) = \sqrt{\frac{\sqrt{[\varepsilon'_j(\omega) - \sin^2\theta]^2 + \varepsilon''^2_j(\omega)} + [\varepsilon'_j(\omega) - \sin^2\theta]}{2}}, \tag{87}$$

*© 2012, V. Lashkaryov Institute of Semiconductor Physics, National Academy of Sciences of Ukraine*

$$\kappa_{z,j}(\omega,\theta) = \sqrt{\frac{\varepsilon_j''^2(\omega)}{2\left\{\sqrt{[\varepsilon_j'(\omega)-\sin^2\theta]^2+\varepsilon_j''^2(\omega)}+[\varepsilon_j'(\omega)-\sin^2\theta]\right\}}}. \quad (88)$$

Two methods exist to calculate light reflection and transmission in the structure. Both give the same result in the case of ideal homogeneous surfaces and interfaces in the structure. In the first method, multiple reflections of the light at surfaces (interfaces) aren't considered explicitly; i.e. amplitudes of all reflected and transmitted waves are supposed to be already included in the amplitudes at the exponents in Eqs. (82) and (83). In the second method, multiple light reflection and transmission at each surface (interface) in the structure are considered explicitly and total reflection (transmission) of the light is calculated as a result of summation of all the components of reflected (transmitted) light.

To calculate transmission and reflection coefficients, entering Eq. (11) for generation function, it is convenient to shift coordinate origin $z = 0$ to the front surface of SC, i.e. to surface air/$SiO_2$ (see Fig. 1). Reflection and transmission for two independent polarizations of incident light are calculated below. In $s$-polarization, the electric field in electromagnetic waves is parallel to the SC surface (i.e. only $y$-components of the electric field are present in $s$-polarized electromagnetic waves), while in $p$-polarization the magnetic field is parallel to the SC surface (i.e. only $y$-components of the magnetic field are present in $p$-polarized electromagnetic waves).

### *7.1. First method for calculation of light reflection (transmission) coefficients*

The first method is the well-known Mueller matrix method. The following general expressions for the electric and magnetic fields $E_y$ and $H_x$ can be written in this case in accordance with the formulae (82), (83) and Maxwell equation $\nabla\times\boldsymbol{E} = -(1/c)d\boldsymbol{H}/dt$ (Gaussian CGS system of units is used) for $s$-polarized electromagnetic waves in materials 1 to 4 (see Fig. 1):

$$E_{y,1} = E_{y,1}^{+}\exp[ik_x x + ik_{z,1}z - i\omega t] + E_{y,1}^{-}\exp[ik_x x - ik_{z,1}z - i\omega t], \quad (89)$$

$$E_{y,2} = E_{y,2}^{+}\exp[ik_x x + ik_{z,2}z - i\omega t] + E_{y,2}^{-}\exp[ik_x x - ik_{z,2}z - i\omega t], \quad (90)$$

$$E_{y,3} = E_{y,3}^{+}\exp[ik_x x + ik_{z,3}(z-d_2) - i\omega t] + E_{y,3}^{-}\exp[ik_x x - ik_{z,3}(z-d_2) - i\omega t], \quad (91)$$

$$E_{y,4} = E_{y,4}^{+}\exp[ik_x x + ik_{z,4}(z-d_2-d_3) - i\omega t], \quad (92)$$

$$H_{x,1} = -N_{z,1}E_{y,1}^{+}\exp[ik_x x + ik_{z,1}z - i\omega t] + N_{z,1}E_{y,1}^{-}\exp[ik_x x - ik_{z,1}z - i\omega t], \quad (93)$$

$$H_{x,2} = -N_{z,2}E_{y,2}^{+}\exp[ik_x x + ik_{z,2}z - i\omega t] + N_{z,2}E_{y,2}^{-}\exp[ik_x x - ik_{z,2}z - i\omega t], \quad (94)$$

$$H_{x,3} = -N_{z,3}E_{y,3}^{+}\exp[ik_x x + ik_{z,3}(z-d_2) - i\omega t] + N_{z,3}E_{y,3}^{-}\exp[ik_x x - ik_{z,3}(z-d_2) - i\omega t], \quad (95)$$

$$H_{x,4} = -N_{z,4}E_{y,4}^{+}\exp[ik_x x + ik_{z,4}(z-d_2-d_3) - i\omega t], \quad (96)$$

where $d_2 = d_{SiO_2}$, $d_3 = d_{ITO}$ (see Fig. 1), $N_{z,j} = \omega k_{z,j}/c$.

We didn't account for the light propagating in negative $z$-direction in expressions (92) and (96), because multiple internal reflections from rear contact are already accounted in the generation function (11) inside a-Si:H layer. Actually, electromagnetic field presentation in the form of (89)-(96) allows to find the intensity $I_0^s(\lambda)\,T_{1\to4}^s(\lambda)$ of light transmitted from vacuum into infinitely thick a-Si:H material ($I_0^s(\lambda)$ is the intensity of incident $s$-polarized light). In the case of finite thickness of a-Si:H layer, $I_0^s(\lambda)\,T_{1\to4}^s(\lambda)$ can be considered as the "first-order" light component generating a series of higher order light components in a-Si:H due to multiple internal light reflections at a-Si:H boundaries. Sum of all these components gives the total intensity of the light in a-Si:H layer in the expression (11) for the generation function.

From the system of boundary conditions

$$E_t\big|_{+} = E_t\big|_{-}, \; H_t\big|_{+} = H_t\big|_{-} \quad (97)$$

for tangential components of electric and magnetic fields at each surface (interface) in the SC structure (signs + and – are introduced here to denote two sides of the same interface) the following relation between amplitudes $E_{y,1}^{+}$, $E_{y,1}^{-}$ in vacuum and $E_{y,4}^{+}$ in a-Si:H can be written:

$$\begin{pmatrix} E_{y,4}^{+} \\ 0 \end{pmatrix} = A_{s+}\hat{M}^{s+}\begin{pmatrix} E_{y,1}^{+} \\ E_{y,1}^{-} \end{pmatrix}, \quad (98)$$

where the coefficient $A_{s+}$ is expressed as

$$A_{s+} = 1/(t_{43}^s t_{32}^s t_{21}^s) \quad (99)$$

and matrix $\hat{M}^{s+}$ as

$$\hat{M}^{s+} = \begin{bmatrix} M_{11}^{s+} & M_{12}^{s+} \\ M_{21}^{s+} & M_{22}^{s+} \end{bmatrix} = \begin{bmatrix} \exp(2ik_{z,3}d_3) & r_{43}^s \\ -r_{34}^s & 1 \end{bmatrix} \times \begin{bmatrix} \exp(2ik_{z,2}d_2) & r_{32}^s \\ -r_{23}^s & 1 \end{bmatrix} \times \begin{bmatrix} 1 & r_{21}^s \\ -r_{12}^s & 1 \end{bmatrix}. \quad (100)$$

The reflection and transmission amplitudes $r_{ij}^s$ ($r_{ji}^s$) and $t_{ij}^s$ ($t_{ji}^s$) relate the amplitudes of reflected $E_{y,i}^{-}$ ($E_{y,j}^{+}$)

*© 2012, V. Lashkaryov Institute of Semiconductor Physics, National Academy of Sciences of Ukraine*

and transmitted $E^{+}_{y,j}\,(E^{-}_{y,i})$ waves with the amplitude $E^{+}_{y,i}\,(E^{-}_{y,j})$ of the incident *s*-polarized wave in a hypothetic case of wave incidence from semi-infinite *i*(*j*)-material onto the interface with semi-infinite *j*(*i*)-material, but for the waves written in the form used in the formulae $(89)-(92)$. In other words, the following explicit expressions for the waves in 1 to 4 materials are used by calculating $r^s_{ij}\,(r^s_{ji})$ and $t^s_{ij}\,(t^s_{ji})$ coefficients (Fig. 7):

$$E^s_{1+} = E^{+}_{y,1}\exp(ik_x x + ik_{z,1}z - i\omega t),\quad E^s_{1-} = E^{-}_{y,1}\exp(ik_x x - ik_{z,1}z - i\omega t);\tag{101}$$

$$E^s_{2+} = E^{+}_{y,2}\exp(ik_x x + ik_{z,2}z - i\omega t),\quad E^s_{2-} = E^{-}_{y,2}\exp(ik_x x - ik_{z,2}z - i\omega t);\tag{102}$$

$$E^s_{3+} = E^{+}_{y,3}\exp[ik_x x + ik_{z,3}(z-d_2) - i\omega t],\quad E^s_{3-} = E^{-}_{y,3}\exp[ik_x x - ik_{z,3}(z-d_2) - i\omega t];\tag{103}$$

$$E^s_{4+} = E^{+}_{y,4}\exp[ik_x x + ik_{z,4}(z-d_2-d_3) - i\omega t],\quad E^s_{4-} = E^{-}_{y,4}\exp[ik_x x - ik_{z,4}(z-d_2-d_3) - i\omega t];\tag{104}$$

$$H^s_{1+} = -N_{z,1}E^{+}_{y,1}\exp[ik_x x + ik_{z,1}z - i\omega t],\quad H^s_{1-} = N_{z,1}E^{-}_{y,1}\exp[ik_x x - ik_{z,1}z - i\omega t];\tag{105}$$

$$H^s_{2+} = -N_{z,2}E^{+}_{y,2}\exp(ik_x x + ik_{z,2}z - i\omega t),\quad H^s_{2-} = N_{z,2}E^{-}_{y,2}\exp(ik_x x - ik_{z,2}z - i\omega t);\tag{106}$$

$$H^s_{3+} = -N_{z,3}E^{+}_{y,3}\exp[ik_x x + ik_{z,3}(z-d_2) - i\omega t],\quad H^s_{3-} = N_{z,3}E^{-}_{y,3}\exp[ik_x x - ik_{z,3}(z-d_2) - i\omega t];\tag{107}$$

$$H^s_{4+} = -N_{z,4}E^{+}_{y,4}\exp[ik_x x + ik_{z,4}(z-d_2-d_3) - i\omega t],\quad H^s_{4-} = N_{z,4}E^{-}_{y,4}\exp[ik_x x - ik_{z,4}(z-d_2-d_3) - i\omega t].\tag{108}$$

From (101)-(108) and boundary conditions at the interfaces (97), the following explicit expressions for the reflection and transmission amplitudes $r^s_{ij}\,(r^s_{ji})$ and $t^s_{ij}\,(t^s_{ji})$ can be obtained:

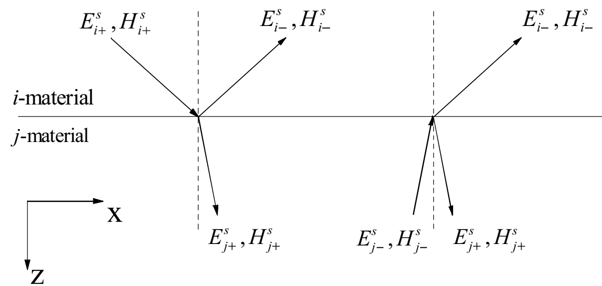


**Fig. 7.** Scheme of electromagnetic wave reflection and transmission by calculating the amplitude coefficients $r^s_{ij}(r^s_{ji})$ and $t^s_{ij}(t^s_{ji})$.

$$r^s_{12} = \frac{E^{-}_{y,1}}{E^{+}_{y,1}} = \frac{N_{z,1}-N_{z,2}}{N_{z,1}+N_{z,2}},\quad r^s_{21} = \frac{E^{+}_{y,2}}{E^{-}_{y,2}} = \frac{N_{z,2}-N_{z,1}}{N_{z,1}+N_{z,2}};\tag{109}$$

$$t^s_{12} = \frac{E^{+}_{y,2}}{E^{+}_{y,1}} = \frac{2N_{z,1}}{N_{z,1}+N_{z,2}},\quad t^s_{21} = \frac{E^{-}_{y,1}}{E^{-}_{y,2}} = \frac{2N_{z,2}}{N_{z,1}+N_{z,2}};\tag{110}$$

$$r^s_{23} = \frac{E^{-}_{y,2}}{E^{+}_{y,2}} = \frac{N_{z,2}-N_{z,3}}{N_{z,2}+N_{z,3}}\exp(2ik_{z,2}d_2),\quad r^s_{32} = \frac{E^{+}_{y,3}}{E^{-}_{y,3}} = \frac{N_{z,3}-N_{z,2}}{N_{z,2}+N_{z,3}};\tag{111}$$

$$t^s_{23} = \frac{E^{+}_{y,3}}{E^{+}_{y,2}} = \frac{2N_{z,2}}{N_{z,2}+N_{z,3}}\exp(ik_{z,2}d_2),\quad t^s_{32} = \frac{E^{-}_{y,2}}{E^{-}_{y,3}} = \frac{2N_{z,3}}{N_{z,2}+N_{z,3}}\exp(ik_{z,2}d_2);\tag{112}$$

$$r^s_{34} = \frac{E^{-}_{y,3}}{E^{+}_{y,3}} = \frac{N_{z,3}-N_{z,4}}{N_{z,3}+N_{z,4}}\exp(2ik_{z,3}d_3),\quad r^s_{43} = \frac{E^{+}_{y,4}}{E^{-}_{y,4}} = \frac{N_{z,4}-N_{z,3}}{N_{z,3}+N_{z,4}};\tag{113}$$

$$t^s_{34} = \frac{E^{+}_{y,4}}{E^{+}_{y,3}} = \frac{2N_{z,3}}{N_{z,3}+N_{z,4}}\exp(ik_{z,3}d_3),\quad t^s_{43} = \frac{E^{-}_{y,3}}{E^{-}_{y,4}} = \frac{2N_{z,4}}{N_{z,3}+N_{z,4}}\exp(ik_{z,3}d_3);\tag{114}$$

With the formally introduced virtual thickness $d_1 = 0$, the expressions (109)-(114) can be rewritten in the following more compact form:

$$r^s_{j,j+1} = \frac{E^{-}_{y,j}}{E^{+}_{y,j}} = \frac{N_{z,j}-N_{z,j+1}}{N_{z,j}+N_{z,j+1}}\exp(2ik_{z,j}d_j),\quad r^s_{j+1,j} = \frac{E^{+}_{y,j+1}}{E^{-}_{y,j+1}} = \frac{N_{z,j+1}-N_{z,j}}{N_{z,j}+N_{z,j+1}};\tag{115}$$

$$t^s_{j,j+1} = \frac{E^{+}_{y,j+1}}{E^{+}_{y,j}} = \frac{2N_{z,j}}{N_{z,j}+N_{z,j+1}}\exp(ik_{z,j}d_j),\quad t^s_{j+1,j} = \frac{E^{-}_{y,j}}{E^{-}_{y,j+1}} = \frac{2N_{z,j+1}}{N_{z,j}+N_{z,j+1}}\exp(ik_{z,j}d_j).\tag{116}$$

With the calculated matrix elements $M^{s+}_{11}$, $M^{s+}_{12}$, $M^{s+}_{21}$ and $M^{s+}_{22}$ of the matrix $\hat{M}^{s+}$ in (98), it is easy to determine the transmission coefficient $T^s_{1\to 4}$ in the generation function (11):

© 2012, V. Lashkaryov Institute of Semiconductor Physics, National Academy of Sciences of Ukraine

$$T^s_{1\to 4} = \mathrm{Re}\left(\frac{S^{s+}_{z,4}}{S^{s+}_{z,1}}\right) = \left| A_{s+} \frac{M^{s+}_{11} M^{s+}_{22} - M^{s+}_{12} M^{s+}_{21}}{M^{s+}_{22}} \right|^2 \mathrm{Re}\left\{\frac{N^*_{z,4}}{N_{z,1}}\right\}, \quad (117)$$

where $S^{s+}_{z,4} = c[\boldsymbol{E}^s_{4,+} \times \boldsymbol{H}^{s*}_{4,+}]_z / 8\pi = E^+_{y,4} \cdot (H^+_{x,4})^* c / 8\pi$ is $z$-component of the energy flux (Poynting vector) in the transmitted $s$-polarized electromagnetic wave in a-Si:H material at the interface ($z = d_2 + d_3$), $S^{s+}_{z,1} = E^+_{y,1} \cdot (H^+_{x,1})^* c / 8\pi$ is $z$-component of the energy flux in the incident $s$-polarized electromagnetic wave in vacuum (air). We use here and in the following expressions like to $\mathrm{Re}(S_{z,i}/S_{z,j})$ instead of $\mathrm{Re}(S_{z,i})/\mathrm{Re}(S_{z,j})$ written in handbooks, because $\mathrm{Re}(S_{z,i}/S_{z,j})$ turns out to be more adequate in the case of absorbing materials. It becomes especially clear if wave transmission and reflection for the wave incidence from absorbing material onto the interface with other material (even non-absorbing) is considered. The energy conservation equality $R + T = 1$ (where $R$ is the wave reflection coefficient and $T$ is the transmission coefficient) is not fulfilled in this case, if expressions like to $\mathrm{Re}(S_{z,i})/\mathrm{Re}(S_{z,j})$ are used, while no such problems arise with expressions like to $\mathrm{Re}(S_{z,i}/S_{z,j})$.

Analogous consideration can be made for $p$-polarized waves and the following connection similar to (98) can be written for the amplitudes $H^+_{y,1}$, $H^-_{y,1}$ in vacuum and $H^+_{y,4}$ in a-Si:H :

$$\begin{pmatrix} H^+_{y,4} \\ 0 \end{pmatrix} = A_{p+} \hat{M}^{p+} \begin{pmatrix} H^+_{y,1} \\ H^-_{y,1} \end{pmatrix}. \quad (118)$$

Expressions for the coefficient $A_{p+}$, matrix $\hat{M}^{p+}$, reflection and transmission amplitudes $r^p_{ij}\,(r^p_{ji})$ and $t^p_{ij}\,(t^p_{ji})$, and transmission coefficient $T^p_{1\to 4}$ are analogous to those written above for the $s$-polarized wave, with the only difference that the Maxwell equation $\nabla \times \boldsymbol{H} = (\varepsilon / c) d\boldsymbol{E} / dt$ has to be used to express $E_x$-components of the electric field in $p$-polarized waves via $H_y$-components of magnetic field, and thus, $\tilde{N}_{z,j} = -N_{z,j} / \varepsilon_j$ has to be substituted everywhere in the formulae (109)-(117) instead of $N_{z,j}$.

To calculate in this approach the reflection coefficient $R^s_{4\to 1}$, the electromagnetic field in vacuum should be written in a form that corresponds to a transmitted wave, while in a-Si:H material in the form of incident and reflected waves, i.e. instead of (89) and (93) the following expressions have to be used:

$$E_{y,1} = E^-_{y,1} \exp[ik_x x - ik_{z,1} z - i\omega t], \quad (119)$$

$$H_{x,1} = N_{z,1} E^-_{y,1} \exp[ik_x x - ik_{z,1} z - i\omega t], \quad (120)$$

while instead of (92) and (96)

$$E_{y,4} = E^+_{y,4} \exp[ik_x x + ik_{z,4}(z - d_2 - d_3) - i\omega t] + E^-_{y,4} \exp[ik_x x - ik_{z,4}(z - d_2 - d_3) - i\omega t] \quad (121)$$

and

$$H_{x,4} = -N_{z,4}\, E^+_{y,4} \exp[ik_x x + ik_{z,4}(z - d_2 - d_3) - i\omega t] + N_{z,4}\, E^-_{y,4} \exp[ik_x x - ik_{z,4}(z - d_2 - d_3) - i\omega t], \quad (122)$$

correspondingly. Then the following equation relating amplitudes of electric fields in vacuum and in a-Si:H can be obtained:

$$\begin{pmatrix} E^-_{y,1} \\ 0 \end{pmatrix} = A_{s-} \hat{M}^{s-} \begin{pmatrix} E^-_{y,4} \\ E^+_{y,4} \end{pmatrix}, \quad (123)$$

where the coefficient $A_{s-}$ is expressed as

$$A_{s-} = 1 / (t^s_{34}\, t^s_{23}\, t^s_{12}) \quad (124)$$

and the matrix $\hat{M}^{s-}$ as

$$\hat{M}^{s-} = \begin{bmatrix} M^{s-}_{11} & M^{s-}_{12} \\ M^{s-}_{21} & M^{s-}_{22} \end{bmatrix} = \begin{bmatrix} \exp(2ik_{z,2} d_2) & -r^s_{21} \\ -r^s_{21} \exp(2ik_{z,2} d_2) & 1 \end{bmatrix} \times \begin{bmatrix} \exp(2ik_{z,3} d_3) & -r^s_{32} \\ -r^s_{32} \exp(2ik_{z,3} d_3) & 1 \end{bmatrix} \times \begin{bmatrix} 1 & -r^s_{43} \\ -r^s_{43} & 1 \end{bmatrix}. \quad (125)$$

The reflection coefficient $R^s_{4\to 1}$ can be expressed as:

$$R^s_{4\to 1} = \mathrm{Re}\left(\frac{S^{s+}_{z,4}}{S^{s-}_{z,4}}\right) = \left| \frac{M^{s-}_{21}}{M^{s-}_{22}} \right|^2, \quad (126)$$

where $S^{s+}_{z,4} = c[\boldsymbol{E}^s_{4,+} \times \boldsymbol{H}^{s*}_{4,+}]_z / 8\pi = E^+_{y,4} \cdot (H^+_{x,4})^* c / 8\pi$ is $z$-component of the energy flux (Poynting vector) in the reflected $s$-polarized electromagnetic wave in a-Si:H material at the interface ($z = d_2 + d_3$), $S^{s-}_{z,4} = c[\boldsymbol{E}^s_{4,-} \times \boldsymbol{H}^{s*}_{4,+}]_z / 8\pi = E^-_{y,4} \cdot (H^-_{x,4})^* c / 8\pi$ is $z$-component of the energy flux in the incident $s$-polarized electromagnetic wave in a-Si:H material at $z = d_2 + d_3$.

An analogous expression can be obtained for the reflection coefficient $R^p_{4\to 1}$ in the case of $p$-polarized electromagnetic waves by using $\tilde{N}_{z,j} = -N_{z,j} / \varepsilon_j$ instead of $N_{z,j}$ in (125), (126) and other related formulae.

The reflection coefficients $R^{s(p)}_{4\to 5}$ in (11) for the electromagnetic wave reflection from rear contact ($j = 5$) can be expressed as

$$R^{s(p)}_{4\to 5} = \left| r^{s(p)}_{45} \right|^2, \quad (127)$$

where

© 2012, V. Lashkaryov Institute of Semiconductor Physics, National Academy of Sciences of Ukraine

$$r_{45}^s = \frac{N_{z,4} - N_{z,5}}{N_{z,4} + N_{z,5}} \ ,$$
$$r_{45}^p = \frac{(N_{z,4} / \varepsilon_4) - (N_{z,5} / \varepsilon_5)}{(N_{z,4} / \varepsilon_4) + (N_{z,5} / \varepsilon_5)} . \quad (128)$$

### *7.2. Second method for calculation of* $R_{4\to1}^{s(p)}$ and $T_{1\to4}^{s(p)}$ *coefficients*

Multiple light reflection and transmission at each surface (interface) in the structure are considered explicitly in this approach, and total reflection (transmission) of light is calculated as a result of summation performed for all the components of reflected (transmitted) light. In approximation of homogeneous front surface of solar cells, the reflection and transmission coefficients $R_{4\to1}^{s(p)}$ and $T_{1\to4}^{s(p)}$ calculated by this method coincide with those obtained by the Mueller matrix method. In the case of non-homogeneous surface, the second method (or, equivalently, "multiple light reflection method") becomes more preferable. For oblique irradiation incidence ($\theta > 0$), the method allows to account for partial metallization of front surface by finger electrodes more exactly, than it is made by introduction of simple shadowing coefficient $(1-m)$ in the generation function (11). To calculate $R_{4\to1}^{s(p)}$ and $T_{1\to4}^{s(p)}$ by the multiple light reflection method, let us first simplify the physical picture of light reflection and transmission in the "vacuum – $SiO_2$ layer – ITO" system (see Fig. 8).

Denote by $r_{13}^{s(p)}$, $r_{31}^{s(p)}$, $t_{31}^{s(p)}$ $t_{31}^{s(p)}$ the amplitudes of reflection and transmission in the "vacuum – top $SiO_2$ layer – ITO" structure considering ITO as semi-infinite medium. These coefficients relate the amplitudes of electric fields (in *s*-polarized waves) and magnetic fields (in *p*-polarized waves) in reflected and transmitted waves with the corresponding amplitudes in the incident waves as shown in Fig. 8. It is easy to obtain from consideration similar to described in the section 6.1 (or by summing the amplitudes of multiple reflected and transmitted waves) the following explicit expressions for these amplitude coefficients:

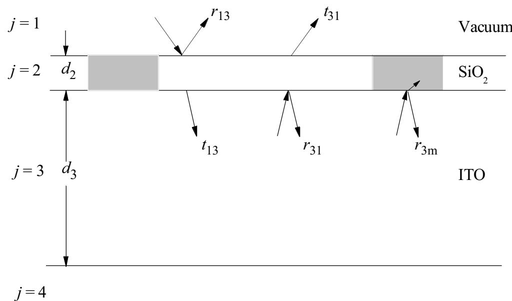


**Fig. 8.** Scheme of light reflection and transmission in the "vacuum – $SiO_2$ layer – ITO" structure for determining the effective amplitudes $r_{13}^s$ $r_{31}^s$, $t_{13}^s$, $t_{31}^s$ used in our subsequent "multiple light reflection method" calculations.

$$r_{13}^{s(p)} = \frac{r_{12}^{s(p)} + r_{23}^{s(p)}}{1 + r_{12}^{s(p)} \cdot r_{23}^{s(p)}} \ ,$$
$$t_{13}^{s(p)} = \frac{t_{12}^{s(p)} \cdot t_{23}^{s(p)}}{1 + r_{12}^{s(p)} \cdot r_{23}^{s(p)}} \ ; \quad (129)$$

$$r_{31}^{s(p)} = \frac{r_{32}^{s(p)} + r_{21}^{s(p)} \exp(2ik_{z,2}d_2)}{1 + r_{12}^{s(p)} \cdot r_{23}^{s(p)}} \ ,$$
$$t_{13}^{s(p)} = \frac{t_{21}^{s(p)} \cdot t_{32}^{s(p)}}{1 + r_{12}^{s(p)} \cdot r_{23}^{s(p)}} \ ; \quad (130)$$

where amplitude coefficients $r_{12}^s, r_{23}^s, t_{12}^s, t_{23}^s, r_{21}^s, r_{32}^s, t_{21}^s, t_{32}^s$ are expressed by the formulae (115), (116), the coefficients $r_{ij}^p$, $t_{ij}^p$ can be obtained from $r_{ij}^s$, $t_{ij}^s$ by substituting $\tilde{N}_{z,j(i)} = -N_{z,j(i)} / \varepsilon_{j(i)}$ instead of $N_{z,j(i)}$ in (115), (116).

After finding the coefficients $r_{13}^{s(p)}$, $r_{31}^{s(p)}$, $t_{31}^{s(p)}$ $t_{31}^{s(p)}$, the equivalent scheme for calculations by using the "multiple light reflections method" in the "vacuum–a-Si:H " structure can be reduced to that shown in Fig. 9 (polarization indices *s* and *p* are omitted in the figure and some following formulae to make them more compact).

Let $L_F$ be the width of finger electrodes at front surface of solar cell (see Fig. 10). Then the distance between edges of adjacent finger electrodes in front surface of SC can be expressed as $L = L_F(1-m)/m$, where *m* is the degree of the surface metallization by finger electrodes. In the case of oblique incidence of irradiation onto SC with finger electrodes on the front surface, the light transmission $T_{1\to4}$ into active a-Si:H region becomes dependent not only on the angle of incidence θ (see Fig. 9), but on the angle ψ between the direction along fingers and the projection of light incidence direction onto the surface (dashed line in Fig. 10), too.

As it follows from Fig. 10, the distance between the edges of adjacent electrodes along the in-plane projection of the direction of light incidence (dashed line) is $\tilde{L} = L / \sin(\psi)$ and the width of shadowed finger regions in this direction is $\tilde{L}_F = L_F / \sin(\psi)$, respectively. The scheme in Fig. 9 corresponds to a cross-section of the SC structure by the plane of light incidence. Thus, the distances between the edges of the shadowed finger regions in Fig. 9 and the width of these regions are just $\tilde{L}$ and $\tilde{L}_F$, respectively. *x*-component of the wave vector in ITO-layer (*j* = 3) is $k_{x,3} = k_{x,1} = (\omega / c)\sin\theta$, while real part of *z*-component of the wave vector is $k_{z,3} = (\omega / c)\, n_{z,3}(\omega,\theta)$, where $n_{z,3}(\omega,\theta)$ is expressed by the formula (87). Thus, for a tangent of wave propagation angle $\theta_3$ in ITO-layer (see Fig. 9) the following formula is valid:

© 2012, V. Lashkaryov Institute of Semiconductor Physics, National Academy of Sciences of Ukraine

$$\tan(\theta_3) = \frac{k_{x,3}}{\mathrm{Re}(k_{z,3})} = \frac{\sin(\theta)}{n_{z,3}(\omega,\theta)}. \quad (131)$$

The optical path $x_d$ along front surface between two subsequent reflections from this surface of the ray reflected from "a-Si:H –ITO" interface (see Fig. 9) can be expressed as

$$x_d = 2d_3 \tan(\theta_3). \quad (132)$$

Thus, within the distance $\tilde{L}_F$ the multiply reflected (from a-Si:H -ITO interface) ray undergoes

$$N_F = \mathrm{integer}(\tilde{L}_F / x_d) + 1 \quad (133)$$

or $N_F - 1$ internal reflections from a metallic finger (depending on the position of ray incidence on SC surface). Let $J_L$ be a number of $x_d$-intervals within the distance $\tilde{L}$ between fingers:

$$J_L = \mathrm{integer}(\tilde{L} / x_d). \quad (134)$$

Let also $x = 0$ be set at the left edge of the right metallic finger in Fig. 9. Then, rays incident from vacuum onto the SC surface within intervals

$$-jx_d < x < -jx_d + \Delta, \quad (135)$$

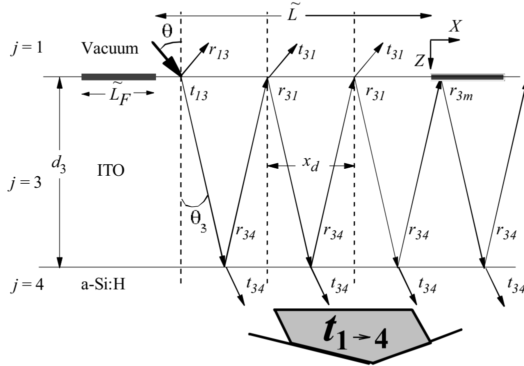


**Fig. 9.** Equivalent scheme of multiple light reflections and transmissions in the "vacuum– a-Si:H" structure for determining the transmission amplitude $t_{1\to4}$ and transmission coefficient $T_{1\to4}$.

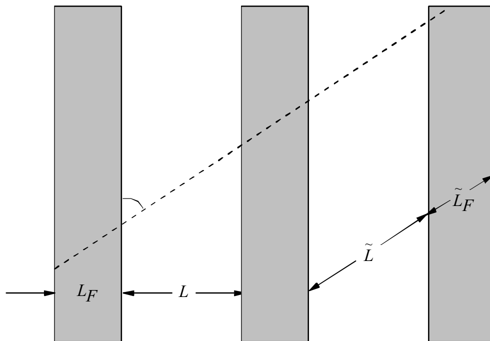


**Fig. 10.** Schematic view of front surface with finger electrodes (shadowed areas). By dashed line the intersection of the plane of light incidence with front surface is shown.

where $j = 1, 2, \ldots J_L$ and $\Delta = \tilde{L}_F - (N_F - 1)\, x_d < x_d$ undergo $N_F$ internal reflections from the right metallic finger in Fig. 9 and $N_F$ or $N_F - 1$ internal reflections from each subsequent finger. However, for the higher order reflections from subsequent fingers really give small contributions to the partial transmission amplitude $t_{1\to4}(j,1)$ of the rays incident in the intervals (135), we consider such rays as being reflected $N_F$ times from each subsequent finger in the structure to facilitate analytical calculations. Then, partial transmission amplitudes $t_{1\to4}(j,1)$ can be written explicitly (see Fig. 9) in the following form:

$$\begin{aligned} t_{1\to4}(j,1) \approx\, & t_{13}t_{34}\Big\{1 + r_{34}r_{31} + (r_{34}r_{31})^2 + \ldots + (r_{34}r_{31})^{j-1} + \\ & + (r_{34}r_{31})^{j-1}\left[r_{34}r_{3m} + (r_{34}r_{3m})^2 + \ldots + (r_{34}r_{3m})^{N_F}\right] + \\ & + (r_{34}r_{31})^{j-1}(r_{34}r_{3m})^{N_F}\left[r_{34}r_{31} + (r_{34}r_{31})^2 + \ldots + (r_{34}r_{31})^{j}\right] + \\ & + (r_{34}r_{31})^{2j-1}(r_{34}r_{3m})^{N_F}\left[r_{34}r_{3m} + (r_{34}r_{3m})^2 + \ldots + (r_{34}r_{3m})^{N_F}\right] + \\ & + (r_{34}r_{31})^{2j-1}(r_{34}r_{3m})^{2N_F}\left[r_{34}r_{31} + (r_{34}r_{31})^2 + \ldots + (r_{34}r_{31})^{j}\right] + \ldots\Big\} = \\ = & \frac{t_{13}t_{34}}{1 - (r_{34}r_{31})^j (r_{34}r_{3m})^{N_F}} \times \\ & \times \left\{\frac{1 - (r_{34}r_{31})^j}{1 - r_{34}r_{31}} + (r_{34}r_{31})^{j-1}\,(r_{34}r_{3m})\frac{1 - (r_{34}r_{3m})^{N_F}}{1 - r_{34}r_{3m}}\right\} = \\ = & \frac{t_{13}t_{34}}{1 - r_{34}r_{31}}\left\{1 + \frac{(r_{34}r_{31})^{j-1}}{1 - (r_{34}r_{31})^j (r_{34}r_{3m})^{N_F}}\,\frac{1 - (r_{34}r_{3m})^{N_F}}{1 - r_{34}r_{3m}}\, r_{34}(r_{3m} - r_{31})\right\}. \end{aligned} \quad (136)$$

Rays incident in the intervals

$$-jx_d + \Delta_1 < x < -(j-1)\, x_d, \quad (137)$$

undergo $N_F - 1$ internal reflections from the right metallic finger in Fig. 9 and $N_F - 1$ or $N_F$ internal reflections from each subsequent finger, so that analogous approximate formula can be written for partial transmission amplitudes $t_{1\to4}(j,2)$ of such rays:

$$\begin{aligned} & t_{1\to4}(j,2) \approx \\ \approx\, & t_{13}t_{34}\Big\{1 + r_{34}r_{31} + (r_{34}r_{31})^2 + \ldots + (r_{34}r_{31})^{j-1} + \\ & + (r_{34}r_{31})^{j-1}\left[r_{34}r_{3m} + (r_{34}r_{3m})^2 + \ldots + (r_{34}r_{3m})^{N_F-1}\right] + \\ & + (r_{34}r_{31})^{j-1}(r_{34}r_{3m})^{N_F-1}\left[r_{34}r_{31} + (r_{34}r_{31})^2 + \ldots + (r_{34}r_{31})^{j}\right] + \\ & + (r_{34}r_{31})^{2j-1}(r_{34}r_{3m})^{N_F-1}\left[r_{34}r_{3m} + (r_{34}r_{3m})^2 + \ldots + (r_{34}r_{3m})^{N_F-1}\right] + \\ & + (r_{34}r_{31})^{2j-1}(r_{34}r_{3m})^{2(N_F-1)}\left[r_{34}r_{31} + (r_{34}r_{31})^2 + \ldots + (r_{34}r_{31})^{j}\right] + \ldots\Big\} = \\ = & \frac{t_{13}t_{34}}{1 - (r_{34}r_{31})^j (r_{34}r_{3m})^{N_F-1}} \times \\ & \times \left\{\frac{1 - (r_{34}r_{31})^j}{1 - r_{34}r_{31}} + (r_{34}r_{31})^{j-1}\,(r_{34}r_{3m})\frac{1 - (r_{34}r_{3m})^{N_F}}{1 - r_{34}r_{3m}} - (r_{34}r_{31})^{j-1}(r_{34}r_{3m})^{N_F}\right\}. \end{aligned} \quad (138)$$

© 2012, V. Lashkaryov Institute of Semiconductor Physics, National Academy of Sciences of Ukraine

The transmission amplitude $t_{1\to4}$ can be expressed as the average of the partial amplitudes (136) and (138) over the distance $J_L x_d$:

$$t_{1\to4} \approx \frac{\sum_{j=1}^{J_L}\left[t_{1\to4}(j,1)\,\Delta + t_{1\to4}(j,2)\,(x_d-\Delta)\right]}{J_L x_d} =$$

$$= \frac{t_{13}t_{34}}{1-r_{34}r_{31}} + \frac{r_{3m}-r_{31}}{r_{31}}\,\frac{1-(r_{34}r_{3m})^{N_F}}{1-r_{34}r_{3m}}\,\frac{t_{13}t_{34}}{1-r_{34}r_{31}}\,\frac{1}{J_L}\times$$

$$\times\left\{\sum_{j=1}^{J_L}\frac{(r_{34}r_{31})^j}{1-(r_{34}r_{31})^j(r_{34}r_{3m})^{N_F}}\right\} - \tag{139}$$

$$-\frac{r_{3m}-r_{31}}{r_{31}}\left(N_F-\frac{\tilde{L}_F}{x_d}\right)\frac{t_{13}t_{34}(r_{34}r_{3m})^{N_F-1}}{1-r_{34}r_{31}}\,\frac{1}{J_L}\times$$

$$\times\left\{\sum_{j=1}^{J_L}\frac{(r_{34}r_{31})^j}{1-(r_{34}r_{31})^j(r_{34}r_{3m})^{N_F}}\,\frac{1-(r_{34}r_{31})^j}{1-(r_{34}r_{31})^j(r_{34}r_{3m})^{N_F-1}}\right\}.$$

In the case of homogeneous front surface ($r_{3m}=r_{31}$), we have from expression (139)

$$t_{1\to4}^{s(p)} = \frac{t_{13}^{s(p)}\,t_{34}^{s(p)}}{1-r_{34}^{s(p)}r_{31}^{s(p)}}\,, \tag{140}$$

which coincides with the result of Mueller matrix method. For computer calculations, the formula (139) can be directly used. However, it is possible to obtain an analytical expression for transmission amplitude $t_{1\to4}$ that gives practically the same result under numerical calculations. To do this, only lowest order multiple internal reflections of the ray from finger electrodes (actually, reflections from the first finger electrode adjacent to the considered interval of light incidence $-J_L x_d < x < 0$) are accounted. After the first electrode, all the internal reflections from front surface are considered as those with the reflection amplitude $r_{31}$ only. In this approximation, we have instead of (136) and (138) the following expressions:

$$t_{1\to4}(j,1)\approx$$
$$\approx t_{13}t_{34}\left\{1+r_{34}r_{31}+(r_{34}r_{31})^2+\ldots+(r_{34}r_{31})^{j-1}+\right.$$
$$+(r_{34}r_{31})^{j-1}\left[r_{34}r_{3m}+(r_{34}r_{3m})^2+\ldots+(r_{34}r_{3m})^{N_F}\right]+$$
$$+(r_{34}r_{31})^{j-1}(r_{34}r_{3m})^{N_F}\left[r_{34}r_{31}+(r_{34}r_{31})^2+\ldots\right]=$$
$$= t_{13}t_{34}\left\{\begin{array}{l}\dfrac{1-(r_{34}r_{31})^j}{1-r_{34}r_{31}} + (r_{34}r_{31})^{j-1}\,(r_{34}r_{3m})\dfrac{1-(r_{34}r_{3m})^{N_F}}{1-r_{34}r_{3m}} + \\ +\dfrac{(r_{34}r_{31})^j\,(r_{34}r_{3m})}{1-r_{34}r_{31}}\end{array}\right\} \tag{141}$$

and

$$t_{1\to4}(j,2)\approx$$
$$\approx t_{13}t_{34}\left\{1+r_{34}r_{31}+(r_{34}r_{31})^2+\ldots+(r_{34}r_{31})^{j-1}+\right.$$
$$+(r_{34}r_{31})^{j-1}\left[r_{34}r_{3m}+(r_{34}r_{3m})^2+\ldots+(r_{34}r_{3m})^{N_F-1}\right]+ \tag{142}$$
$$+(r_{34}r_{31})^{j-1}(r_{34}r_{3m})^{N_F-1}\left[r_{34}r_{31}+(r_{34}r_{31})^2+\ldots\right]=$$
$$= t_{13}t_{34}\left\{\begin{array}{l}\dfrac{1-(r_{34}r_{31})^j}{1-r_{34}r_{31}} + (r_{34}r_{31})^{j-1}\,(r_{34}r_{3m})\dfrac{1-(r_{34}r_{3m})^{N_F}}{1-r_{34}r_{3m}} - \\ -(r_{34}r_{31})^{j-1}(r_{34}r_{3m})^{N_F} + \dfrac{(r_{34}r_{31})^j(r_{34}r_{3m})^{N_F-1}}{1-r_{34}r_{31}}\end{array}\right\},$$

respectively.

Calculating the sum in (139) with partial amplitudes (141) and (142), the following analytical expression can be obtained for the transmission amplitude $t_{1\to4}$:

$$t_{1\to4}\approx\frac{t_{13}\,t_{34}}{1-r_{34}r_{31}}+$$
$$+t_{13}\,t_{34}\,r_{34}(r_{3m}-r_{31})\frac{1-(r_{34}r_{3m})^{N_F}}{1-r_{34}r_{3m}}\left\{\frac{1}{J_L}\frac{1-(r_{34}r_{31})^{J_L}}{1-r_{34}r_{31}}\right\}-$$
$$-\frac{r_{3m}-r_{31}}{r_{3m}}\left(N_F-\frac{\tilde{L}_F}{x_d}\right)\frac{t_{13}t_{34}(r_{34}r_{3m})^{N_F}}{1-r_{34}r_{31}}\left\{\frac{1}{J_L}\frac{1-(r_{34}r_{31})^{J_L}}{1-r_{34}r_{31}}\right\}, \tag{143}$$

which also transforms into the result of Mueller matrix method for homogeneous front surface ($r_{3m}=r_{31}$).

Transmission coefficients for electromagnetic energy fluxes $T_{1\to4}^s$ and $T_{1\to4}^p$, which enter into the expression (11) for the generation function, are expressed using the above described method of multiple light reflections as

$$T_{1\to4}^s=\mathrm{Re}\left[\frac{N_{z,4}}{N_{z,1}}\right]\left|t_{1\to4}^s\right|^2 \text{ and } T_{1\to4}^p=\mathrm{Re}\left[\frac{\tilde{N}_{z,4}}{\tilde{N}_{z,1}}\right]\left|t_{1\to4}^p\right|^2, \tag{144}$$

where $\tilde{N}_{z,j}=-N_{z,j}/\varepsilon_j$.

Similar consideration for the electromagnetic waves incident from a-Si:H material onto "vacuum-ITO" structure allows to obtain the following expression for the reflection amplitudes $r_{4\to1}^{s(p)}$ (analog of the expression (139) for the transmission amplitudes $t_{1\to4}^{s(p)}$):

$$r_{4\to1}\approx r_{43}+\frac{t_{43}\,r_{31}t_{34}}{1-r_{34}r_{31}}+$$
$$+\frac{r_{3m}-r_{31}}{r_{31}}\,\frac{1-(r_{34}r_{3m})^{N_F}}{1-r_{34}r_{3m}}\,\frac{t_{43}\,r_{31}t_{34}}{1-r_{34}r_{31}}\,\frac{1}{J_L}\times$$
$$\times\left\{\sum_{j=1}^{J_L}\frac{(r_{34}r_{31})^j}{1-(r_{34}r_{31})^j(r_{34}r_{3m})^{N_F}}\right\}- \tag{145}$$
$$-\frac{r_{3m}-r_{31}}{r_{31}}\left(N_F-\frac{\tilde{L}_F}{x_d}\right)\frac{t_{43}\,r_{31}t_{34}(r_{34}r_{3m})^{N_F-1}}{1-r_{34}r_{31}}\,\frac{1}{J_L}\times$$
$$\times\left\{\sum_{j=1}^{J_L}\frac{(r_{34}r_{31})^j}{1-(r_{34}r_{31})^j(r_{34}r_{3m})^{N_F}}\,\frac{1-(r_{34}r_{31})^j}{1-(r_{34}r_{31})^j(r_{34}r_{3m})^{N_F-1}}\right\}.$$

© 2012, V. Lashkaryov Institute of Semiconductor Physics, National Academy of Sciences of Ukraine

The approximate analytical expression for $r_{4\to1}^{s(p)}$, numerical values of which practically coincide with those of the more exact expression (145), looks like

$$r_{4\to1} \approx r_{43} + \frac{t_{43}\, r_{31}\, t_{34}}{1-r_{34}r_{31}} +$$
$$+ t_{43}\, r_{31}\, t_{34}\, r_{34}(r_{3m}-r_{31}) \frac{1-(r_{34}r_{3m})^{N_F}}{1-r_{34}r_{3m}} \left\{ \frac{1}{J_L} \frac{1-(r_{34}r_{31})^{J_L}}{1-r_{34}r_{31}} \right\} -$$
$$- \frac{r_{3m}-r_{31}}{r_{3m}} \left( N_F - \frac{\tilde{L}_F}{x_d} \right) \frac{t_{43}\, r_{31}\, t_{34} (r_{34}r_{3m})^{N_F}}{1-r_{34}r_{31}} \left\{ \frac{1}{J_L} \frac{1-(r_{34}r_{31})^{J_L}}{1-r_{34}r_{31}} \right\}. \quad (146)$$

This expression is analogous to the expression (143) for the transmission amplitude $t_{1\to4}$.

Reflection coefficients for electromagnetic energy fluxes $R_{4\to1}^{s(p)}$, which enter the expression (11) for the generation function, are expressed in the method described above for multiple light reflections as

$R_{4\to1}^{s(p)} = \left| r_{4\to1}^{s(p)} \right|^2$. (147)

In an extraordinary case of extremely oblique light incidence (when $J_L$ probably can turn to zero), latter $J_L$-containing terms in the formulae (139), (143), (145), (146) should be omitted. Thus, in this case reflection and transmission become "homogeneous" (i.e. coinciding with that of Mueller matrix method) like to that in the cases of normal ray incidence or incidence along fingers. The reason is that only rare high order $r_{3m}$-terms can possibly enter the total reflection and transmission sums in this case, which practically cannot distort "homogeneous" reflection and transmission, described by first terms in the above formulae.

The reflection coefficients $R_{4\to5}^{s(p)}$ in (11) are given by the formula (127).

## 7. Calculation of the angle θ of sun rays incidence onto SC and the angle ψ between the direction along fingers and projection of the light incidence direction onto SC surface as functions of time and SC local orientation

In a local coordinate system with $z$-axis directed along the line from Earth center (i.e. perpendicularly to horizontal Earth surface at the site, where SC is mounted), $x$-axis directed strongly to west and $y$-axis to south (Northern hemisphere is considered) orientation of a unit vector $\boldsymbol{e}_s$ directed to Sun can be characterized by the zenith angle $\theta_s$ (altitude or elevation angle $\beta_s$) and azimuth angle $\varphi_s$, see Fig. 11. Time dependence of the zenith angle $\theta_s$ (or elevation angle $\beta_s$) can be expressed by the following formula (see [8, 9]):

$$\cos(\theta_s) = \sin(\beta_s) =$$
$$= \cos(\alpha)\cos(\varepsilon)\cos\left[\frac{2\pi}{T_e}\left(t - \frac{T_e}{2}\right)\right] + \sin(\alpha)\sin(\varepsilon), \quad (148)$$

where $T_e = 24$ hours is the nominal solar day duration, $t$ is the local daytime starting at midnight ($0 \le t \le T_e$), $\alpha$ is latitude of a site where SC is mounted ($0 \le \alpha \le 90°$), $\varepsilon$ is the Earth's declination angle, which, in its turn, is the function of the day number $T(D)$ in a year ($1 \le T(D) \le 365$),

$$\varepsilon = \left(\frac{23.45°}{180°}\pi\right)\sin\left(\frac{T}{365}2\pi\right) =$$
$$= 0.40928 \cdot \sin(0.0172142 \cdot T) = \quad (149)$$
$$= -0.40928 \cdot \cos\left[0.0172142 \cdot (D+10)\right].$$

In the formula (149), $T$ is the day number starting from March 22, while $D$ is the day number starting from January 1.

For each day in a year, sunrise and sunset times $t_1$ and $t_2$ can be determined from the condition $\cos(\theta_s) = 0$:

$$t_{1,2} = \frac{T_e}{2} \mp T_e \frac{\arccos[-\tan(\alpha)\tan(\varepsilon)]}{2\pi}. \quad (150)$$

Thus, maximal possible period $\Delta t$ of SC operation in the day is determined by the difference $t_2 - t_1$:

$$\Delta t = T_e \frac{\arccos[-\tan(\alpha)\tan(\varepsilon)]}{\pi}. \quad (151)$$

If $\theta_s(t,T)$ is found from (148), the time dependence of the azimuth angle $\varphi_s(t,T)$ can be determined using the following formula [8, 9]:

$$\cos(\varphi_s) = -\frac{\cos(\varepsilon)\sin\left[2\pi(t - T_e/2)/T_e\right]}{\sin(\theta_s)}. \quad (152)$$

Let $\boldsymbol{n}_m$ be unit vector characterizing SC orientation in local coordinate system shown in Fig. 11 ($\boldsymbol{n}_m$ is directed along the normal to SC surface). For the following calculations, we introduce new coordinate system $\{X_m, Y_m, Z_m\}$, connected with the solar cell and characterized by unit vectors $\boldsymbol{e}_{x_m}$ (directed along the highway in the site of SC mounting), $\boldsymbol{e}_{y_m}$ (lying in the SC plane and perpendicular to $\boldsymbol{e}_{x_m}$) and $\boldsymbol{e}_{z_m} = \boldsymbol{n}_m$ (see Fig. 12).

Components of these unit vectors in the local coordinate system shown in Fig. 10 are given by the following formulae:

$$\boldsymbol{e}_{x_m} = \{-\sin\varphi_m, \cos\varphi_m, 0\}, \quad (153)$$
$$\boldsymbol{e}_{y_m} = \{-\cos\theta_m \cos\varphi_m, -\cos\theta_m \sin\varphi_m, \sin\theta_m\} \quad (154)$$
$$\boldsymbol{e}_{z_m} = \{\sin\theta_m \cos\varphi_m, \sin\theta_m \sin\varphi_m, \cos\theta_m\}. \quad (155)$$

The unit vector $\boldsymbol{e}_s$ in the local coordinate system $\{X, Y, Z\}$ shown in Fig. 10 has the components

$$\boldsymbol{e}_s = \{\sin\theta_s \cos\varphi_s, \sin\theta_s \sin\varphi_s, \cos\theta_s\}. \quad (156)$$

© 2012, V. Lashkaryov Institute of Semiconductor Physics, National Academy of Sciences of Ukraine

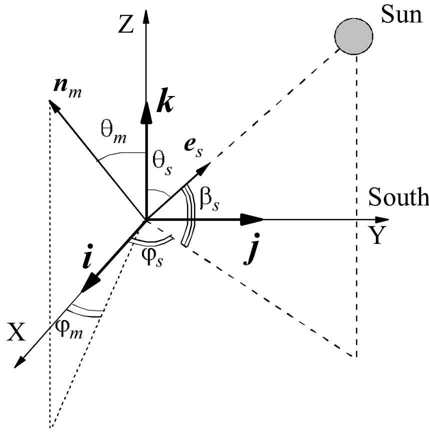


**Fig. 11.** Local coordinate system and angles characterizing sun and solar cell orientations in the local coordinate system.

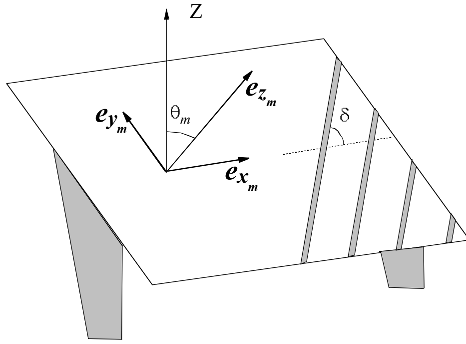


**Fig. 12.** SC-based coordinate system formed by three unit vectors $e_{x_m}$, $e_{y_m}$ and $e_{z_m}$.

Using (155) and (156), we can find now the time dependence $\theta(t,T)$ of the angle of incidence of (direct) solar rays onto SC surface at local geographical site and for local SC orientation (reflection and transmission coefficients, calculated in Sec. 6, depend just on this angle):

$$\begin{aligned}&\boldsymbol{e}_{z_m}\cdot\boldsymbol{e}_s=|\boldsymbol{e}_{z_m}||\boldsymbol{e}_s|\cos\theta=\cos\theta=\\&=\sin\theta_m\cos\varphi_m\sin\theta_s\cos\varphi_s+\\&+\sin\theta_m\sin\varphi_m\sin\theta_s\sin\varphi_s+\cos\theta_m\cos\theta_s.\end{aligned}\tag{157}$$

The daytime $t_1'$ ($t_1\le t_1'\le t_2$) at which irradiation of SC front surface by direct solar rays starts and the daytime $t_2'$ ($t_1'\le t_2'\le t_2$) at which the direct irradiation falls to zero (and, respectively, period $t_2'-t_1'$ of SC functioning in this day) can be found from the condition $\cos\theta=0$.

Let $\delta$ be the angle characterizing orientation of finger electrodes on SC front surface relatively to $\boldsymbol{e}_{x_m}$ direction (see Fig. 12). To determine the angle between $X_m$-axis and the plane of light incidence (or, in other words, between $X_m$-axis and projection of light propagation direction onto the SC surface), we consider the vector product

$$\boldsymbol{v}=[\boldsymbol{e}_{z_m}\times\boldsymbol{e}_s]=|\boldsymbol{e}_{z_m}||\boldsymbol{e}_s|\sin\theta_{sm}\,\boldsymbol{e}_{vm}=\sin\theta_{sm}\,\boldsymbol{e}_{vm},\tag{158}$$

where $\theta_{sm}$ is the angle between unit vectors $\boldsymbol{e}_{z_m}$ and $\boldsymbol{e}_s$. It is evident that both $\boldsymbol{e}_{z_m}$ and $\boldsymbol{e}_s$ vectors lie in the plane of light incidence. For this reason, the vector $\boldsymbol{v}$ and unit vector $\boldsymbol{e}_{vm}=\boldsymbol{v}/v$ lie in the SC plane that is normal to the plane of light incidence. Using decomposition (155) of the unit vector $\boldsymbol{e}_{z_m}$ over the unit vectors $\boldsymbol{i},\boldsymbol{j},\boldsymbol{k}$ (see Fig. 11) and analogous decomposition (156) for the unit vector $\boldsymbol{e}_s$, we have from (158)

$$\begin{aligned}&\boldsymbol{v}=v_x\boldsymbol{i}+v_y\boldsymbol{j}+v_z\boldsymbol{k}=\\&=(\sin\theta_m\sin\varphi_m\cos\theta_s-\cos\theta_m\sin\theta_s\sin\varphi_s)\boldsymbol{i}+\\&+(\cos\theta_m\sin\theta_s\cos\varphi_s-\sin\theta_m\cos\varphi_m\cos\theta_s)\boldsymbol{j}+\\&+(\sin\theta_m\cos\varphi_m\sin\theta_s\sin\varphi_s-\sin\theta_m\sin\varphi_m\sin\theta_s\cos\varphi_s)\boldsymbol{k}.\end{aligned}\tag{159}$$

Thus,

$$\sin\theta_{sm}=v=\sqrt{v_x^2+v_y^2+v_z^2},\tag{160}$$

where explicit expressions for the components $v_x$, $v_y$ and $v_z$ are written in the formula (159). Analogously, for the unit vector $\boldsymbol{e}_{vm}=\boldsymbol{v}/v$ the following formula is valid

$$\begin{aligned}&\boldsymbol{e}_{vm}=e_{vm,x}\boldsymbol{i}+e_{vm,y}\boldsymbol{j}+e_{vm,z}\boldsymbol{k}=\\&=(\sin\theta_m\sin\varphi_m\cos\theta_s-\cos\theta_m\sin\theta_s\sin\varphi_s)/\sin\theta_{sm}\,\boldsymbol{i}+\\&+(\cos\theta_m\sin\theta_s\cos\varphi_s-\sin\theta_m\cos\varphi_m\cos\theta_s)/\sin\theta_{sm}\,\boldsymbol{j}+\\&+(\sin\theta_m\cos\varphi_m\sin\theta_s\sin\varphi_s-\sin\theta_m\sin\varphi_m\sin\theta_s\cos\varphi_s)/\sin\theta_{sm}\,\boldsymbol{k}.\end{aligned}\tag{161}$$

The angle $\varphi_{vx_m}$ between $\boldsymbol{e}_{vm}$ and $\boldsymbol{e}_{x_m}$ vectors lying in the SC plane can be easily found from the well-known formula for the scalar product of vectors:

$$\boldsymbol{e}_{vm}\cdot\boldsymbol{e}_{x_m}=|\boldsymbol{e}_{vm}||\boldsymbol{e}_{vm}|\cos(\varphi_{vx_m})=\cos(\varphi_{vx_m}).\tag{162}$$

Using (153) and (161), we find that

$$\cos(\varphi_{vx_m})=-\sin\varphi_m\,e_{vm,x}+\cos\varphi_m\,e_{vm,y},\tag{163}$$

where explicit expressions for the components $e_{vm,x}$ and $e_{vm,y}$ are written in the formula (161). As the vector $\boldsymbol{e}_{vm}$ is perpendicular to the plane of light incidence, the angle $\psi_{sx}$ between the $X_m$-axis and projection of light incidence direction onto the SC surface is expressed as follows:

$$\psi_{sx}=\pi/2-\varphi_{vx_m}.\tag{164}$$

© 2012, V. Lashkaryov Institute of Semiconductor Physics, National Academy of Sciences of Ukraine

The angle $\psi$ between the direction along fingers and the light incidence direction projection onto the SC surface is expressed, respectively, as

$$\psi = \psi_{sx} - \delta . \quad (165)$$

The reflection and transmission coefficients calculated in Sec. 6.2 by using the "multiple reflection method" depend just on this angle.

## 9. Optical constants of materials in SC structure

Optical constants of materials in the structure can be presented in the form of complex dielectric permittivity $\varepsilon_j(\omega) = \varepsilon'_j(\omega) + i\varepsilon''_j(\omega)$, or complex refractive index $N_j(\omega) = \sqrt{\varepsilon_j(\omega)} = n_j(\omega) + i\kappa_j(\omega)$. It is evident that between $\varepsilon'_j(\omega), \varepsilon''_j(\omega)$ and $n_j(\omega)$, $\kappa_j(\omega)$ values, relations $\varepsilon'_j = n_j^2 - \kappa_j^2$ and $\varepsilon''_j = 2n_j\kappa_j$ exist. So, if we have data describing $n_j(\omega)$ and $\kappa_j(\omega)$ dependences, we can easily find $\varepsilon'_j(\omega)$ and $\varepsilon''_j(\omega)$ dependences and vice versa. In the cases, when the wavelength $\lambda$ is argument of the optical constants instead of the frequency $\omega$, the dependences $\varepsilon_j(\omega)$ and $N_j(\omega)$ can be easily obtained using the relationship $\omega = 2\pi c/\lambda$ between the photon frequency and wavelength or, equivalently, $\hbar\omega = 2\pi\hbar c/\lambda$ between the photon energy $\hbar\omega$ and wavelength. The latter relationship can be rewritten in the well-known numerical form $\hbar\omega = 1.239842/\lambda \approx 1.24/\lambda$ for the case of energy $\hbar\omega$ expressed in electronvolts and the wavelength $\lambda$ expressed in micrometers.

### *9.1. Dielectric permittivity of the top $SiO_2$ layer*

We have used for fused $SiO_2$ material permittivity Sellmeier analytic function from the work [10]:

$$\varepsilon_{SiO_2}(\lambda) = 1.4923 + \frac{0.61497\,\lambda^2}{\lambda^2 - (0.115)^2} - 0.01059\,\lambda^2 , \quad (166)$$

where the wavelength $\lambda$ is expressed in micrometers. As noted in [10], this analytical formula gives very precise values of the $SiO_2$ permittivity in the energy range below 5.8 eV, practically coinciding with tabulated experimental values in Palic's handbook [11].

### *9.2. Refraction index of the indium tin oxide (ITO) layer*

Data of the work [12] for real ($n$) and imaginary ($\kappa$) parts of ITO refraction index have been used. Wavelength dependences of $n$ and $\kappa$ in ITO in the actual wavelength range are shown in Fig. 13. Points represent data of the work [12], solid curves are splines constructed and used in our program.

### *9.3. Permittivity of the a-Si:H layer*

Data of the work [13] for real and imaginary parts of a-Si:H material permittivity have been used. Energy dependences of $\varepsilon'$ and $\varepsilon''$ in the actual energy range (plotted on the base of these data) are shown in Fig. 14 (for comparison, filled squares for $\varepsilon'(E)$ -dependence at [H] = 0 are the data of the work [13]). As it clear from the figure, permittivity in this case depends on the hydrogen content [H], too. For this reason, in our program two-dimensional splines (i.e. on energy and hydrogen content) based on the data of the work [13] have been constructed and used for numerical calculations. The absorption coefficient $\alpha_\lambda$ of a-Si:H material in the generation function (11) is expressed as $\alpha_\lambda = 2\kappa_{z,4}(\omega,\theta)\,\omega/c$, where $\kappa_{z,4}(\omega,\theta)$ is given by the formula (88) ($j = 4$ in this formula corresponds to a-Si:H layer in our notation, see Fig. 1). In band bending calculations (see Eq. (79)), we have used the value $\varepsilon = 16.5 - 0.3\cdot[\mathrm{H}]$ for static permittivity of a-Si:H, where [H] is hydrogen content (in %) in a-Si:H. This $\varepsilon([\mathrm{H}])$-dependence corresponds to data of the work [14].

### *9.4. Dielectric permittivity of metal contact electrodes on SC surfaces*

Aluminum was considered as a metal, from which contact electrodes on back and front surface of SC are formed. In our calculations, we have used the wavelength dependences of real and imaginary parts of the permittivity for pure aluminum presented in [11, 15], see Fig. 15.

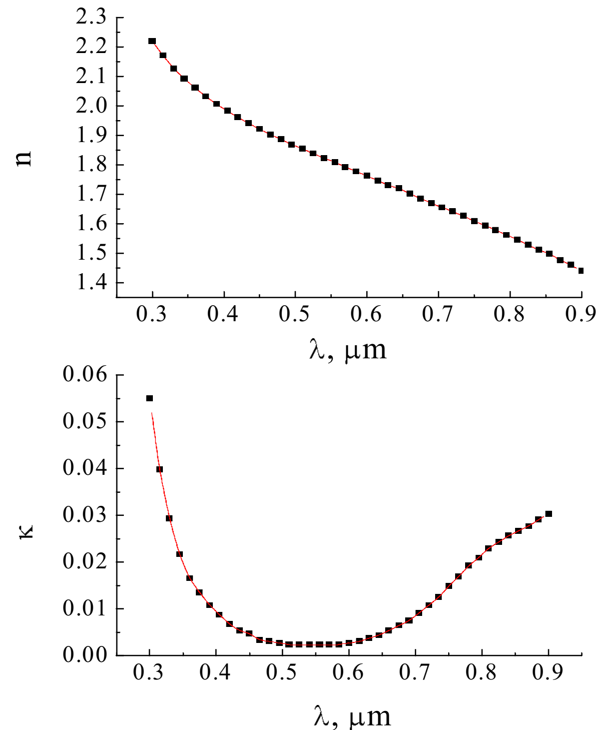


**Fig. 13.** Real ($n$) and imaginary ($\kappa$) parts of the complex refractive index of indium tin oxide (ITO).

© 2012, V. Lashkaryov Institute of Semiconductor Physics, National Academy of Sciences of Ukraine

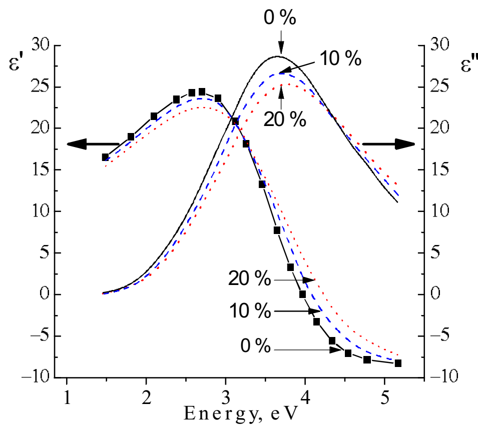


**Fig. 14.** Real and imaginary parts of the complex dielectric permittivity of hydrogenated amorphous silicon. Hydrogen content in % is marked for each curve.

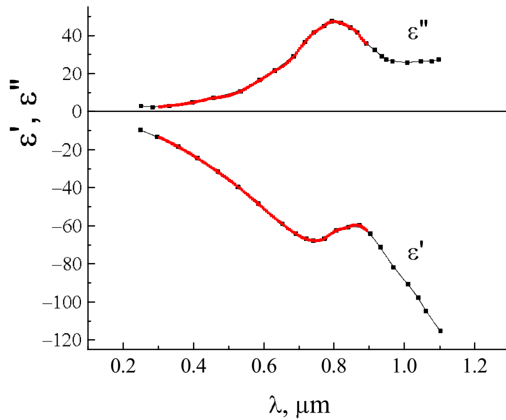


**Fig. 15.** Real and imaginary parts of the complex dielectric permittivity of pure aluminum.

## 10. Solar radiation spectra

In our calculations, we have used standard solar radiation spectra AM0 corresponding to space conditions outside Earth atmosphere and standard (ASTM G-173) reference solar radiation spectra of sunlight at the Earth surface AM1.5D and AM1.5G (at AM1.5 conditions length of the path of light through the atmosphere is 1.5 times that of the shorter path when the sun is directly overhead) [16]. The spectrum AM1.5D corresponds to direct radiation from Sun and AM1.5G to "global" radiation, which includes both direct and diffuse radiation. These spectra are shown in Fig. 16.

## 11. Solar cell efficiency and other related parameters

To calculate the efficiency and other parameters of a-Si:H solar cells in different time moments, to which different light incidence angles θ and "finger-plane of incidence" angles ψ correspond (see Figs 9 and 10), or to calculate SC parameters averaged over different time intervals (daytime, year, etc.), we have to know solar spectra for arbitrary positions of Sun, i.e. for arbitrary atmosphere masses AM. In principle, it can be done using the data of the work by Christian Gueymard [17]. In the applied FORTRAN program, SC efficiencies and other parameters can be calculated only for the case of normal light incidence onto SC surface for irradiation conditions AM0 and AM1.5. Nevertheless, the general formulae are written below, accounting for possible *s*- and *p*-polarized parts of incident light in the case of oblique incidence.

The total density of short-circuit current, as pointed earlier, can be calculated by summing the contributions from all vanishingly small (i.e. practically monochromatic) parts of solar spectra $I(\lambda)$ shown in Fig. 16:

$$j_{SC} = \frac{1}{2}\int_{\lambda_m}^{\lambda_0} \Im(\lambda)\left[\left(j_{e,SC}^{\lambda,s} + j_{h,SC}^{\lambda,s}\right) + \left(j_{e,SC}^{\lambda,p} + j_{h,SC}^{\lambda,p}\right)\right] d\lambda, \quad (167)$$

where $\lambda_m$ is the shortest wavelength in solar spectrum, at which light penetration into active region of SC still occurs ($\lambda_m = 0.31$ μm value corresponding to the energy 4.0 eV has been used in the calculations, for sign conversion of the real part of a-Si:H permittivity at the energy close to 4.0 eV, see Fig. 14), $\lambda_0$ is the wavelength corresponding to the a-Si:H bandgap energy $E_g$ (or, more exactly, to mobility edge energy $E_m$, which can be somewhat lower than $E_g$ due to possible electron and hole transport via conduction and valence band tail states), $\Im(\lambda) = I(\lambda)/\hbar\omega = I(\lambda)\lambda/(2\pi\hbar c)$ is the spectral density of photons, incident onto unit area, $j_{e,SC}^{\lambda,s(p)}$ and $j_{h,SC}^{\lambda,s(p)}$ are the considered in Sections 2 and 3 electron and hole contributions into the short-circuit current from monochromatic light with the wavelength λ. Unit light intensities $I_0^{p(s)}(\lambda)$ in the formulae (11), (13) and (32) have to be used by calculating the current densities $j_{e,SC}^{\lambda,s(p)}$ and $j_{h,SC}^{\lambda,s(p)}$ for the integrand expression in (167). Instead of $I_0^{p(s)}(\lambda)$ in (11), (13) and (32) the intensity $\Im(\lambda)\,d\lambda/2$ for *s*-polarized part of light and the same $\Im(\lambda)\,d\lambda/2$ intensity for *p*-polarized part of the light appears in (167).

The photocurrent density under SC circuit loading can be expressed as a sum of the irradiation-induced short-circuit current density $j_{SC}$ and the density of exponential diode current flowing in the opposite direction:

$$j_{ph}(V) = j_{SC} - j_s\left[\exp(eV/rkT) - 1\right], \quad (168)$$

where $V$ is the voltage drop across the load, saturation current density $j_s$ and non-ideality factor $r$ are the diode characteristics of $p-i(n)$ junction in a-Si:H. Values $j_s = 10^{-12}$ A/cm and $r = 1.5$ have been used in our calculations [18].

© 2012, V. Lashkaryov Institute of Semiconductor Physics, National Academy of Sciences of Ukraine

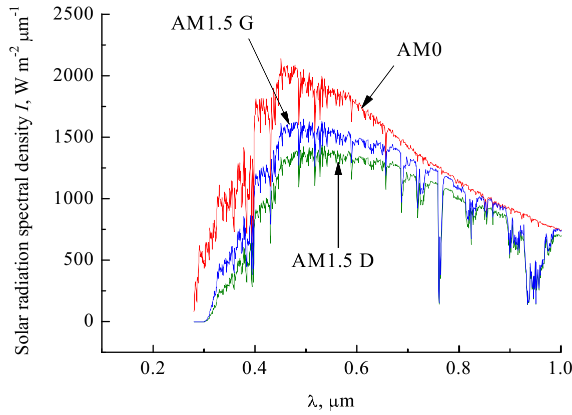


**Fig. 16.** Standard solar radiation spectra $I(\lambda)$ in the actual range of wavelengths.

The open-circuit voltage $V_{oc}$ can be found from (168) by using the condition $j_{ph}(V_{oc}) = 0$:

$$V_{oc} = \frac{rkT}{e}\ln\left[\frac{j_{SC}}{j_s}+1\right]. \qquad (169)$$

*11.1. SC parameters in an ideal case of zero internal resistance*

In a hypothetic case of ideal SC possessing zero internal resistivity, the power generated by the unit area of solar cell is expressed as

$$W = V j_{ph}(V) = V j_s[\exp(eV_{oc}/rkT) - \exp(eV/rkT)]. \qquad (170)$$

The consumed power achieves maximal value $W_m$ at an optimal load, when condition

$$\left.\frac{dW}{dV}\right|_{V=V_m} = 0 \qquad (171)$$

is fulfilled. As it follows from (170) and (171), the voltage $V_m$ in the optimal regime can be found from the equation

$$\exp\left(\frac{eV_m - eV_{oc}}{rkT}\right)\left[\frac{eV_m}{rkT}+1\right] - 1 = 0. \qquad (172)$$

The optimal density of photocurrent in this case is expressed as

$$j_m = j_s\frac{eV_m}{rkT}\exp\left(\frac{eV_m}{rkT}\right), \qquad (173)$$

and the optimal power generated by the unit area of SC as

$$W_m = V_m j_m = j_s\frac{eV_m^2}{rkT}\exp\left(\frac{eV_m}{rkT}\right). \qquad (174)$$

The product of optimal load resistance $R_m$ on SC area $S$ is expressed, respectively, as

$$R_m S = \frac{V_m}{j_m} = \frac{rkT}{ej_s}\exp\left(-\frac{eV_m}{rkT}\right). \qquad (175)$$

We characterize SC by three types of its efficiency. The efficiency $\eta_a$ is the relation of power $W_m$ collected from the unit SC area in an optimal regime (174) to the power absorbed inside active a-Si:H layer of the SC $W_a$ (this absorbed power is only a part of the total solar irradiation power incident on SC due to above described limitations of the spectral range as well as due to partial reflection of light and its absorption in metallic contacts and non-active layers of the SC structure):

$$\eta_a = \frac{W_m}{W_a}. \qquad (176)$$

The absorbed power can be easily calculated by integrating the sum of generation functions (11) $g^s(z,\lambda) + g^p(z,\lambda)$ (with $I(\lambda)\,d\lambda/2$ instead of $I_0^p(\lambda)$ and $I_0^s(\lambda)$) over the thickness of active a-Si:H layer and over the spectral range $\lambda_m..\lambda_0$ like to that in (167).

The efficiency $\eta_p$ is the relation of the power $W_m$ collected from the unit SC area in an optimal regime to the incident irradiation power $W_p$ within the spectral interval $\lambda_m..\lambda_0$ (due to this limitation of the spectral range, $W_p$ is only a part of total solar irradiation power incident on SC):

$$\eta_p = \frac{W_m}{W_p}. \qquad (177)$$

By its definition, the power $W_p$ by the can be calculated as

$$W_p = \int_{\lambda_m}^{\lambda_0} I(\lambda)\,d\lambda. \qquad (178)$$

Finally, the efficiency $\eta$ is the relation of power $W_m$ collected from the unit SC area in an optimal regime to the incident irradiation power $W$ within the whole spectral range of solar irradiation:

$$\eta = \frac{W_m}{W}, \qquad (179)$$

where the power $W$ can be calculated analogously to $W_p$:

$$W = \int_0^{\infty} I(\lambda)\,d\lambda. \qquad (180)$$

In practice, $\lambda_l = 0.28$ µm can be used instead of zero as the lower edge of solar spectrum in the integral (180) and $\lambda_u = 4$ µm as the upper edge, because electromagnetic waves outside this spectral region practically do not contribute to the total power $W$.

© 2012, V. Lashkaryov Institute of Semiconductor Physics, National Academy of Sciences of Ukraine

Once more parameter, characterizing SC, is the filling factor $F$ defined as

$$F = \frac{W_m}{V_{oc}\, j_{SC}} . \quad (181)$$

*11.2. SC parameters with an account of SC series photoresistance and ohmic power losses at the contact finger grid on the front SC surface*

Consider active a-Si:H region of SC as a series of vanishingly small parts with a length $dz$. Each of such parts can be characterized by the resistance $dR$

$$dR = \frac{dz}{\sigma(z)\, S} , \quad (182)$$

where $S$ is the solar cell area, $\sigma(z)$ is the conductivity depending on the free carrier concentrations $p(z)$ and $n(z)$ in valence and conduction bands, respectively:

$$\sigma(z) = e[n(z)\mu_n(z) + p(z)\mu_p(z)] , \quad (183)$$

where $\mu_{n(p)}$ are the hole (electron) mobilities. In our approach, the mobilities are considered as parameters of the model. They are supposed to be constants across $p$- or $i(n)$- region of a-Si:H (but probably having different values in these regions). I.e., we characterize $p$-region by the electron and hole mobilities $\mu_n^{(p)}$ and $\mu_p^{(p)}$ as well as $i(n)$-region by $\mu_n^{i(n)}$ and $\mu_p^{i(n)}$, respectively.

For the $i(n)$-part of a-Si:H layer beyond space charge region, we can write

$$n(z) = \Delta n(z) + n_n , \quad p(z) = p_n , \quad (184)$$

where $n_n$ is an equilibrium concentration of major carriers (electrons) in $i(n)$-region, which in accordance with (73) and (74) is expressed as

$$n_n = \nu_c \exp\left( \frac{E_F^{i(n)} - E_g}{kT} \right) . \quad (185)$$

The energy $E_F^{i(n)}$ in (185) is the Fermi level energy counted from the valence band edge in $i(n)$-region in the absence of irradiation. This energy has been determined earlier under band bending calculations (as well as the Fermi level energy $E_F^p$ in $p$-region of a-Si:H layer), see Sections 4 and 5. The concentration $\Delta n(z)$ of photoelectrons in $i(n)$-region can be expressed as a sum of all contributions from vanishingly small monochromatic parts of the incident irradiation spectra:

$$\Delta n(z) = \tau_n^{i(n)} \int_{\lambda_m}^{\lambda_0} \frac{g^s(z,\lambda) + g^p(z,\lambda)}{2} \Im(\lambda)\, d\lambda , \quad (186)$$

where $\tau_n^{i(n)}$ is the lifetime of photoelectrons in this region, $g^{s(p)}$ are the generation functions (11) with the unit intensities $I_0^{s(p)}(\lambda)$ (actually, in the formula (186) the intensity $\Im(\lambda)\, d\lambda / 2$ appears instead of the monochromatic intensities $I_0^p(\lambda)$ and $I_0^s(\lambda)$ in the formula (11)). This expression for the concentration of excess major carriers in $i(n)$-region is a consequence of the generation-recombination balance equation

$$\frac{\Delta n^{s(p)}(z,\lambda)}{\tau_n^{i(n)}} = g^{s(p)}(z,\lambda) . \quad (187)$$

As compared with the analogous balance equation (10) for photoelectrons in $p$-region, the diffusion term is absent in (187) because electrons generated in $i(n)$-region don't contribute to the diffusion photocurrent (they cannot overcome $p - i(n)$ junction barrier and are left $i(n)$-region, thus increasing the conductivity of this region). Non-equilibrium excess holes in this region form corresponding part of the diffusion photocurrent (see Sec. 3). Actually, they serve as an external source of current (in addition to non-equilibrium excess electrons in $p$-region) and for this reason should be excluded from the system of carriers responsible for ohmic losses in this region. Thus, according to (75) and (76) we can write the following expression for equilibrium part of the hole concentration in $i(n)$-region contributing to the conductivity in $z$-direction in this region:

$$p(z) = p_n = \nu_v \exp\left( -\frac{E_F^{i(n)}}{kT} \right) . \quad (188)$$

Analogously, for the $p$-part of a-Si:H layer beyond space charge region we can write

$$n(z) = n_p , \quad p(z) = p_p + \Delta p(z) , \quad (189)$$

where $p_p$ is the equilibrium concentration of major carriers (holes) in $p$-region, which in accordance with (75) and (76) is expressed as

$$p_p = \nu_v \exp\left( -\frac{E_F^p}{kT} \right) . \quad (190)$$

The energy $E_F^p$ in (190) is the Fermi level energy counted from the valence band edge in $p$-region in absence of irradiation. The concentration $\Delta p(z)$ of excess photoholes in $p$-region can be expressed like to (186) as

$$\Delta p(z) = \tau_p^{(p)} \int_{\lambda_m}^{\lambda_0} \frac{g^s(z,\lambda) + g^p(z,\lambda)}{2} \Im(\lambda)\, d\lambda , \quad (191)$$

where $\tau_p^{(p)}$ is the lifetime of excess photoholes in this region. According to (73) and (74), we can write the following expression for the electron concentration that contributes to the conductivity in $p$-region:

$$n(z) = n_p = \nu_c \exp\left( \frac{E_F^p - E_g}{kT} \right) . \quad (192)$$

As to the space charge region at $p - i(n)$ junction, we somewhat simplify our consideration and evaluate its

*© 2012, V. Lashkaryov Institute of Semiconductor Physics, National Academy of Sciences of Ukraine*

contribution into the internal SC series resistance using equilibrium values of carrier concentrations (i.e. corresponding to the case when irradiation is absent and no voltage drops at an external load) instead of the total carrier concentrations that can be obtained using the formulae (21) and (41):

$$n(z) = n_n \exp[y(z)] \ , \quad p(z) = p_p \exp[-y(z) - y_{pn}] \ , \quad (193)$$

where concentrations $n_n$ and $p_p$ are expressed by the formulae (185) and (190). Thus, we overestimate the contribution of SCR to the total internal resistance, because under irradiation and an external load the SCR thickness will be less than $z_p + z_n$ (thickness in the equilibrium case) and the carrier concentrations in SCR will be higher. However, due to relatively small contribution of SCR into the total series resistance in many practical cases (because of smallness of the SCR thickness as compared with the total a-Si:H thickness) this overestimation would not be too critical. Thus, SC efficiencies would be somewhat larger than those calculated within this approximation.

Substituting (184), (189) or (193) into (183) and integrating (182) over a-Si:H thickness, we obtain thus the following internal series resistance (photoresistance) of the a-Si:H layer of SC:

$$R = \frac{1}{S}\left[\int_0^{d_p - z_p} \frac{dz}{\sigma(z)} + \int_{d_p - z_p}^{d_p + z_n} \frac{dz}{\sigma(z)} + \int_{d_p + z_n}^{d_p + d} \frac{dz}{\sigma(z)}\right]. \quad (194)$$

Besides a-Si:H layer, the ITO layer with the contact grid also should contribute to the ohmic losses. According to the results of works [19, 20], the ITO-contact grid resistance can be expressed in the following form:

$$R_g = \frac{V_{oc}}{S j_{SC}}\left[1 - \frac{2L_c}{L}\tan\left(\frac{L}{2L_c}\right)\right], \quad (195)$$

where $L = L_F(1-m)/m$ is the distance between fingers in the contact grid (see Fig. 10), $L_F$ – width of finger electrodes, $m$ – degree of front surface metallization by electrodes, $L_c$ – characteristic effective length of hole collection by electrodes:

$$L_c = \left(e\mu_p^{ITO} n_p^{ITO} d_{ITO} V_{oc} / j_{SC}\right)^{1/2}. \quad (196)$$

In the formula (196), $\mu_p^{ITO}$ is the hole mobility in ITO, $n_p^{ITO}$ – hole concentration in ITO (as high values as $9.61\cdot10^{18}$ cm$^{-3}$ are reported for the hole concentration in ITO [21]), $d_{ITO} = d_3$ – ITO layer thickness (see Fig. 1).

Thus, the total internal series resistance of solar cell $R_{SC}$ can be expressed as

$$R_{SC} = R + R_g \,. \quad (197)$$

With an account of internal ohmic losses, the expression (168) for the photocurrent takes up the following form:

$$\begin{aligned} j_{ph}(V) &= j_{SC} - j_s\left\{\exp\left[\frac{eV + ej_{ph}(V)SR_{SC}}{rkT}\right] - 1\right\} = \\ &= j_s\left\{\exp\left[\frac{eV_{oc}}{rkT}\right] - \exp\left[\frac{eV + ej_{ph}(V)SR_{SC}}{rkT}\right]\right\}, \end{aligned} \quad (198)$$

where $V$ is the a voltage drop at an external load.

For the net power consumed by the external load, we have now the following expression instead of (170):

$$\begin{aligned} W &= Vj_{ph}(V) = \\ &= V j_s\left\{\exp\left[\frac{eV_{oc}}{rkT}\right] - \exp\left[\frac{eV + ej_{ph}(V)SR_{SC}}{rkT}\right]\right\}. \end{aligned} \quad (199)$$

The net power achieves its maximal value at a voltage $V_m$, which can be found from the evident condition

$$\frac{dW}{dV} = j_{ph}(V) + V\frac{d\,j_{ph}}{dV} = 0\,. \quad (200)$$

Going to dimensionless quantities $v = V/V_{oc}$, $i = j_{ph}/j_0$, $w = W/(j_0 V_{oc}) = v\cdot i(v)$, $\rho = ej_0R_{SC}S/(rkT)$ and $u = eV_{oc}/rkT$, where $j_0 = j_s\exp[eV_{oc}/(rkT)]$, we can rewrite formulae (198) and (200) in the form of the following system of two transcendental equations for the dimensionless current density $i$ and voltage $v$ dropping at optimal external load:

$$f_1(i,v) = \exp[\rho i + u(v-1)] + i - 1 = 0\,, \quad (201)$$

$$f_2(i,v) = \frac{dw}{dv} = i(v) + v\frac{di}{dv} = 0\,. \quad (202)$$

It follows from (201) that

$$df_1 = \frac{df_1}{di}di + \frac{df_1}{dv}dv = 0\,, \quad (203)$$

i.e.

$$\frac{di}{dv} = -\frac{df_1/dv}{df_1/di} = -\frac{u\exp[\rho i + u(v-1)]}{\rho\exp[\rho i + u(v-1)] + 1}\,. \quad (204)$$

Substituting (204) into (202), we obtain

$$\begin{aligned} f_2(i,v) &= i(v) + v\frac{di}{dv} = \\ &= \frac{(\rho i - uv)\exp[\rho i + u(v-1)] + i}{\rho\exp[\rho i + u(v-1)] + 1} = 0. \end{aligned} \quad (205)$$

For $\exp[\rho i + u(v-1)] > 0$, we can divide both parts of Eq. (201) by this exponential function. Analogously, as both the photocurrent density $i$ and denominator $\rho\exp[\rho i + u(v-1)] + 1$ in (205) differ from zero, we can divide both parts of Eq. (205) by these values, too. Thus, the following two equations can be used to determine the optimal photocurrent and net voltage instead of (201) and (205):

© 2012, V. Lashkaryov Institute of Semiconductor Physics, National Academy of Sciences of Ukraine

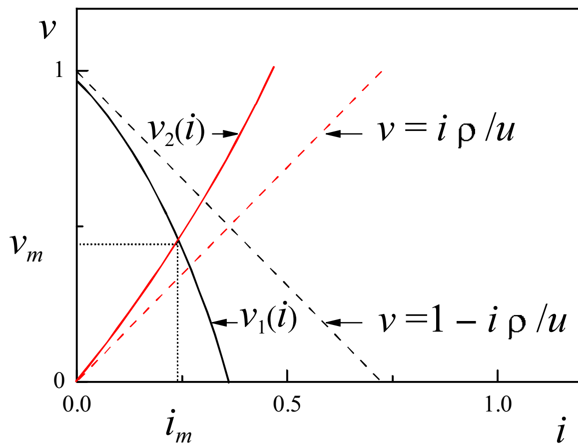


**Fig. 17.** Schematic graphical solution of Eqs.(206) and (207).

$$\tilde{f}_1(i,v) = 1 + \frac{i-1}{\exp[\rho i + u(v-1)]} = 0\,, \qquad (206)$$

$$\tilde{f}_2(i,v) = \frac{(uv-\rho i)}{i}\exp[\rho i + u(v-1)] - 1 = 0\,. \qquad (207)$$

Finding the intersection point of the solution $v_1(i)$ of (206) with the solution $v_2(i)$ of (207) (see Fig. 17), we determine the dimensionless optimal photocurrent density $i_m$ and dimensionless net voltage $v_m$.

Knowing the optimal photocurrent density $j_m = j_0 i_m$ and optimal net voltage $V_m = V_{oc} v_m$, we can calculate all the parameters characterizing SC (using the formulae (174)-(181)) with account for internal series photoresistance and contact grid resistance.

## 12. Conclusions

In this paper, we presented a detailed theory of photoconversion in structures based on a-Si:H . Its use helps to illustrate the dependence of the photoconversion efficiency on the key physical parameters and to optimize the value of photovoltaic parameters. This allows to obtain high values of the efficiency of the discussed solar cells.

*References*


1. M.J. Powell and S.C. Deane, Improved defect-pool model for charged defects in amorphous silicon // *Phys. Rev. B*, **48**, No.15, 10815 (1993).
2. M.J. Powell and S.C. Deane, Defect-pool model and the hydrogen density of states in hydrogenated amorphous silicon // *Phys. Rev. B*, **53**, No.15, p. 10121 (1996).
3. C. Longeaud, J.A. Schmidt, and R.R. Koropecki, Determination of semiconductor band gap state parameters from photoconductivity measurements. II. Experimental results // *Phys. Rev. B*, **73**, No.23, 235317 (2006).
4. L. Ley, Band tails of a-Si:H: photoemission and absorption data, in: *Properties of Amorphous Silicon and its Alloys*, ed. by Tim Searle (University of Sheffield, UK). Publ. by INSPEC, The Institution of Electrical Engineers, London, UK, 1998, p. 113.
5. Jianjun Liang, E.A. Schiff, S. Guha, Baojie Yan, and J. Yang, Hole-mobility limit of amorphous silicon solar cells // *Appl. Phys. Lett.* **88**, 063512 (2006); Parameter Values for Modeling Photocarrier Processes in Hydrogenated Amorphous Silicon, *http://physics.syr.edu/~schiff/AMPS/SU_Parameter_Suggestions.html*
6. Wataru Futako, Toshio Kamiya, Charles M. Fortmann, Isamu Shimizu, The structure of 1.5±2.0 eV band gap amorphous silicon prepared by chemical annealing // *J. Non-Cryst. Solids*, **266-269**, p. 630 (2000).
7. Saad M. Malik, Stephen K. O'Leary, An analysis of the distributions of electronic states associated with hydrogenated amorphous silicon // *J. Mater. Sci: Materials in Electronics*, **16**, p. 177 (2005).
8. Biometeorology, ESPM 129, Lecture 9, Solar Radiation, Part 2, Earth-Sun Geometry, *http://nature.berkeley.edu/biometlab/espm129/pdf/Lecture%209%20espm%20129.pdf*
9. Solar Concepts, *http://www.usc.edu/dept/architecture/mbs/tools/vrsolar/Help/solar_concepts.html*
10. C.M. Herzinger, B. Johs, W.A. McGahan, J.A. Woollam, W. Paulson, *Elipsometric determination of optical constants for silicon and thermally grown silicon dioxide via a multi-sample, multi-wavelength, multi-angle investigation*, J. Appl. Phys. **83**, No. 6, 3323 (1998).
11. *Handbook of Optical Constants of Solids*, ed. by E.D. Palic. Academic Press, New York, 1997, p. 749.
12. H. Hoppe, N.S. Sariciftci and D. Meissner, Optical constants of conjugated polymer/fullerene based bulk-heterojunction organic solar cells // *Mol. Cryst. Liquid Cryst.* **385**, [233]/113 (2002).
13. S.H. Lin, Y.C. Chan, D.P. Webb, Y.W. Lam, Investigation of mis-estimation of structure of amorphous silicon in ellipsometric modelling // *J. Non-Cryst. Solids*, **276**, p. 35 (2000).
14. A.H. Mahan, Structural information on a-Si:H from IR and Raman spectroscopy, in: *Properties of Amorphous Silicon and its Alloys*, ed. by Tim Searle (University of Sheffield, UK). Publ. by INSPEC, The Institution of Electrical Engineers, London, UK, 1998, p. 39.


*© 2012, V. Lashkaryov Institute of Semiconductor Physics, National Academy of Sciences of Ukraine*

15. Lance W. Barron, Jason Neidrich, Santosh K. Kurinec, Optical, electrical, and structural properties of sputtered aluminum alloy thin films with copper, titanium and chromium additions // *Thin Solid Films*, **515**, p. 3363 (2007).
16. *http://rredc.nrel.gov/solar/spectra/am1.5/ASTMG173.html*
17. Christian Gueymard, SMARTS2: A Simple Model of the Atmospheric Radiative Transfer of Sunshine: algorithms and performance assessment, (1995) // *http://www.fsec.ucf.edu/en/publications/pdf/FSEC-PF-270-95.pdf*
18. R.A. Street, *Hydrogenated Amorphous Silicon.* Cambridge University Press, 1991.
19. A.V. Sachenko, A.I. Shkrebtii, T.V. Panichevskaya, Theoretical model of solar cell with contact grid // *Optoelektronika i poluprovodnikovaya tekhnika*, **21**, p. 63 (1991), in Russian.
20. A.V. Sachenko, A.V. Gorban’, On the collection of photocurrent in solar cells with a contact grid // *Semiconductor Physics, Quantum Electronics and Optoelectronics*, **2**, No.2, p. 42 (1999).
21. Chen Chen, Zhenguo Ji, Chao Wang, Lina Zhao, Qiang Zhou, P-type tin–indium oxide films prepared by thermal oxidation of metallic InSn alloy films // *Mater. Lett.* **60**, p. 3096 (2006).


*© 2012, V. Lashkaryov Institute of Semiconductor Physics, National Academy of Sciences of Ukraine*